Journal Pre-proofs

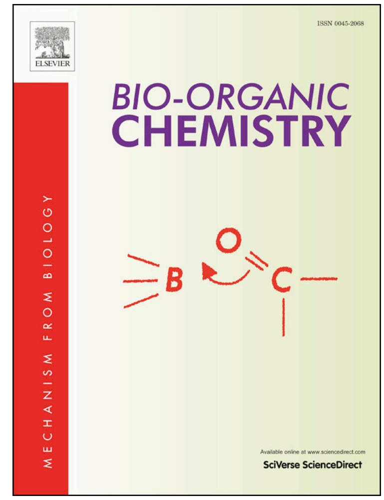

Discovery of Diaminopyrimidine-carboxamide Derivatives as JAK3 Inhibitors

Rajesh Bahekar, Nandini Panchal, Shubhangi Soman, Jigar Desai, Dipam Patel, Anil Argade, Archana Gite, Sanjay Gite, Bhaumin Patel, Jeevan Kumar, Sachchidanand S, Harilal Patel, Rajesh Sundar, Abhijit Chatterjee, Jogeswar Mahapatra, Hoshang Patel, Krishnarup Ghoshdastidar, Debdutta Bandyopadhyay, Ranjit C. Desai

PII: S0045-2068(19)32066-8
DOI: https://doi.org/10.1016/j.bioorg.2020.103851
Reference: YBIOO 103851

To appear in: *Bioorganic Chemistry*

Received Date: 4 December 2019
Revised Date: 10 April 2020
Accepted Date: 12 April 2020

Please cite this article as: R. Bahekar, N. Panchal, S. Soman, J. Desai, D. Patel, A. Argade, A. Gite, S. Gite, B. Patel, J. Kumar, S. S, H. Patel, R. Sundar, A. Chatterjee, J. Mahapatra, H. Patel, K. Ghoshdastidar, D. Bandyopadhyay, R.C. Desai, Discovery of Diaminopyrimidine-carboxamide Derivatives as JAK3 Inhibitors, *Bioorganic Chemistry* (2020), doi: https://doi.org/10.1016/j.bioorg.2020.103851

Discovery of Diaminopyrimidine-carboxamide Derivatives as JAK3 Inhibitors#

Rajesh Bahekar [a,*], Nandini Panchal [a,b], Shubhangi Soman [b,*], Jigar Desai [a], Dipam Patel [a], Anil Argade [a], Archana Gite [a], Sanjay Gite [a], Bhaumin Patel [a], Jeevan Kumar [c], Sachchidanand S [c], Harilal Patel [d], Rajesh Sundar [d], Abhijit Chatterjee [d], Jogeswar Mahapatra [d], Hoshang Patel [e], Krishnarup Ghoshdastidar [e], Debdutta Bandyopadhyay [e] and Ranjit C. Desai[a]

[a] Department of Medicinal Chemistry, Zydus Research Centre, Sarkhej-Bavla, N.H. 8A Moraiya, Ahmedabad 382210, India.
[b] Department of Chemistry, Faculty of Science, M.S. University of Baroda, Vadodara 390002, India.
[c] Department of Bioinformatics, Zydus Research Centre, Sarkhej-Bavla, N.H. 8A Moraiya, Ahmedabad 382210, India.
[d] Department of Pharmacology, Zydus Research Centre, Sarkhej-Bavla, N.H. 8A Moraiya, Ahmedabad 382210, India.
[e] Department of Cell Biology, Zydus Research Centre, Sarkhej-Bavla, N.H. 8A Moraiya, Ahmedabad 382210, India.

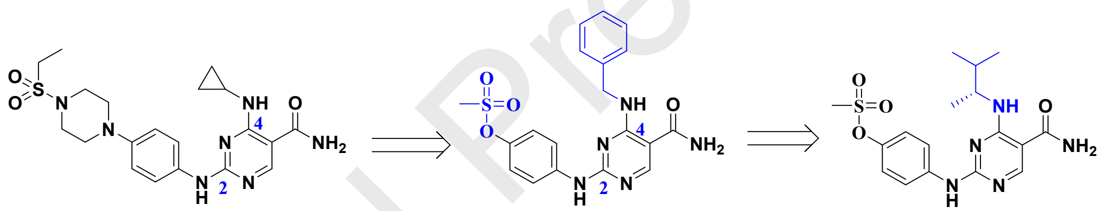

ABSTRACT

Selective inhibition of janus kinase (JAK) has been identified as an important strategy for the treatment of autoimmune disorders. Optimization at the C2 and C4-positions of pyrimidine ring of Cerdulatinib led to the discovery of a potent and orally bioavailable 2,4-diaminopyrimidine-5-carboxamide based JAK3 selective inhibitor (**11i**). A cellular selectivity study further confirmed that **11i** preferentially inhibits JAK3 over JAK1, in JAK/STAT signaling pathway. Compound **11i** showed good anti-arthritic activity, which could be correlated with its improved oral bioavailability. In the repeat dose acute toxicity study, **11i** showed no adverse changes related to gross pathology and clinical signs, indicating that the new class JAK3 selective inhibitor could be viable therapeutic option for the treatment of rheumatoid arthritis.

#ZRC communication No: 596 *(Part of Ph.D thesis work of Nandini Panchal).*

*Corresponding author: Rajesh Bahekar: Tel.: +91-2717-665555; Fax: +91-2717-665355
E-mail: rajeshbahekar@zyduscadila.com (Rajesh Bahekar)

1. Introduction

Rheumatoid arthritis (RA) is a chronic inflammatory disease characterized by synovitis and joint destruction. [1-2] The multiple cytokines (tumor necrosis factor-α (TNF-α) and interleukin (IL)) triggers RA pathogenesis by inducing intracellular signal transduction, via JAK/STAT (Janus kinases and signal transducers and activators of transcription) signaling pathway. [3-6] The JAK family of enzymes (JAK1, JAK2, JAK3 and tyrosine kinase 2 (TYK2)) are cytoplasmic protein tyrosine kinases, associated with various cytokine-mediated signal transduction pathways. [7-9] Binding of the cytokines to their corresponding receptors induces JAK activation and subsequent phosphorylation. [10] The activated JAKs phosphorylate STAT proteins, which translocate to the nucleus and promote cytokine-responsive gene expression. [11] Due to unique role of JAKs in the immune system, inhibition of JAKs emerged out as one of the most validated and attractive therapeutic target for the treatment of autoimmune disorders such as RA and other inflammatory diseases. [12]

JAK3 is expressed in lymphoid cells, drives pro-inflammatory signaling cascades, inducing cytokine expression in the synovial fibroblasts, activated monocytes and macrophages. [13] JAK3 pairs with the JAK1 and it is involved in common gamma chain (γc) cytokine (IL-2, IL-4, IL-7, IL-9, IL-15 and IL-21) signaling pathways, which play important role in the T-cell differentiation, proliferation and survival. [14]

Clinically, JAK1 inhibition induces undesirable secondary pharmacodynamic effects such as cholesterol and liver enzyme elevation. [15] JAK2 mediates signaling via hematopoietic cytokines such as erythropoietin (EPO), thus dose-limiting tolerability and safety issues such as anemia are being associated with the JAK2 inhibition. [16] Selective JAK3 inhibition only deters common gamma (γc) chain receptors signaling and spares JAK1 dependent immunoregulatory cytokines (IL-10, IL-27 and IL-35). [17] Thus, JAK3 selective inhibitors are likely to offer a better efficacy to the safety ratio in the clinic for the treatment of chronic inflammatory disorders.

2. Result and discussion

2.1. Design of novel JAK inhibitor:

Over the past decades, structurally diverse JAK inhibitors were identified containing pyrrolo [2,3-b]pyridine and pyrimidine core as a promising scaffold (Fig. 1). [18-20] Tofacitinib, a low nanomolar (nM) JAK3 inhibitor but limited selectivity against JAK1 and JAK2 (Fig. 1) and the Baricitinib, a dual JAK1 and JAK2 inhibitor are approved for the treatment of RA. [21, 22] Momelotinib, a dual JAK1 and JAK2 inhibitor and the Fedratinib, a JAK2 selective inhibitor are under clinical trials, for the treatment of myelofibrosis. [23, 24] A reversible ATP-competitive dual SYK/JAK inhibitor, Cerdulatinib is under clinical trial for the treatment of leukemia and lymphoma. [25] Knowing the potential side effects associated with the PAN JAK inhibitors, efforts are being directed towards the development of a JAK3 selective inhibitor, for an effective treatment of autoimmune disorder. [26]

Recently, JAK3 selective inhibitor programs have targeted covalent bond formation with Cys909 as an optimization strategy, including PF-06651600, an irreversible covalent inhibitor of JAK3 (Fig. 1), which is in the clinical trials for the treatment of inflammatory diseases. [27-29] Most of the irreversible JAK3 inhibitors demonstrated good JAK3 enzymatic selectivity but largely lacked cellular selectivity or appropriate physicochemical properties to be tested *in vivo*. [30]

In this article, we present our efforts to develop novel non-covalent inhibitors of the JAK3. It was hypothesized that the non-covalent JAK3 selective inhibitors could be devoid of systemic toxicity. An approach undertaken to overcome the JAK isozymes selectivity was to capitalize on the amino acid sequence differences among the JAKs, more specifically to favor hydrogen bonding interaction with the JAK3 cysteine (Cys-909) residue in the catalytic domain to develop the novel, non-covalent JAK3 selective inhibitor. While designing JAK3 inhibitors, attempts were made to avoid an introduction of the covalent reactive groups (CRGs), in the structural features to circumvent the possibility of a covalent modification of Cys-909.

Structural modifications were carried out in the Cerdulatinib (having pyrimidine moiety as a key pharmacophore, Fig. 1). In the docking studies (Fig. 3) Cerdulatinib showed hydrogen bonding interactions in the hinge region of JAK3 enzyme but no hydrogen bonding was observed in the catalytic domain. Initial attempts involved maintaining essential hydrogen bonding interactions in the original scaffold and optimization at the C2-position of pyrimidine ring of Cerdulatinib to induce additional hydrogen bonding with the Cys-909. Modifications at the C2 position of pyrimidine ring in the C4 benzylated Cerdulatinib (Set-1, Table 1) led to the single digit nM potent compound **5k**, with moderate isoform selectivity (Table 3). Docking study of **5K** reveals no additional hydrogen bonding in the catalytic domain of the JAK3.

In the second set (Table 2), changes were carried out at the C4-position of the **5k**, mainly to improve JAK3 isoform selectivity, which led to the discovery of a novel 2,4-diaminopyrimidine-5-carboxamide based JAK3 selective inhibitor **11i**. Docking study of **11i** showed additional hydrogen bonding with the Cys-909 of JAK3 (Fig. 3) and no interaction with the Serine residue of JAK isoforms, in the ATP binding pockets. Based on the *in vitro* results, highly potent and selective compound (**11i**) was assessed *in vivo* for the pharmacokinetic (PK), efficacy and animal toxicity studies.

2.2. Chemistry:

Synthesis of 2, 4-diaminopyrimidine-5-carboxamides derivatives (**5a-o** and **11a-o)** was carried out as depicted in Scheme **1** and **2**, following the modified literature procedure. [31] Treatment of ethyl 4-chloro-2-(methylthio)-pyrimidine-5-carboxylate (**1**) with benzyl amine gave 4-benzylamino carboxylate, followed by hydrolysis, to get the acid moiety (**2**). Compound **2** was converted into amide (**3**), using HOBt and EDC.HCl, followed by reaction with aq. ammonia. Compound **3** converted to reactive methyl sulfinyl derivate (**4**) using *m*-CPBA, followed by treatment with substituted aryl amines furnished compounds **5a-o**. For the synthesis of **11a-o**, substituted 4-hydroxy pyrimidine-5-carboxylate (**6**) was converted to reactive methyl sulfinyl derivate, using *m*-CPBA, followed by treatment with 4-aminophenylmethanesulfonate to get intermediate **7**, which was converted to acid (**8**), using LiOH, as a base. Acid functionality of compound **8** transformed to amide (**9**), using aq. ammonia. Phenolic hydroxyl group of compound **9** was activated into reactive chloro group (**10**), using $POCl_3$, followed by reaction with substituted amines, furnished compounds **11a-o**.

Compounds **5a-o** and **11a-o** were prepared in good yield (60 to 80%), under the mild reaction condition. Spectral data were found to be in conformity with the structures assigned, which ensure the formation of compounds **5a-o** and **11a-o** (see experimental section, 4.2).

2.3. JAK3 inhibitory activity (enzyme based biochemical screening):

For *in vitro* JAK3 inhibitory activity screening, Cerdulatinib and Tofacitinib were used as a positive control. In Set-1 (Table 1), 2-substituted diaminopyrimidine-5-carboxamides (**5a-o**) analogues displayed varying degree of JAK3 inhibitory activities. *m*-substituted *N*-phenyl derivatives, **5a** (*m*-aniline), **5b** (oxopropanamide), **5c** (oxoaceticacid), **5d** (cinnamamide), **5e** (methanesulfonamide), **5f** (sulfoximine) and **5g** (sulfonylacetamide) showed moderate JAK3 inhibitory activity (IC_{50}: > 120 nM). Compounds **5h** and **5i** (positional isomer of **5e** and **5f**) exhibited enhanced JAK3 inhibitory activity (IC_{50}: 56 and 48 nM). Compound **5j** (acetyl protection of **5h**) displayed moderate JAK3 activity (IC_{50}: 102 nM). Replacement of the sulfonamide group (**5h**) with methane sulfonate (**5k**, IC_{50}: 9.5 nM) and iso-propyl sulfonate (**5l**, IC_{50}: 22.4 nM) led to higher JAK3 inhibitory activity, whereas *o*-substitution with the electron donating groups such as amino (**5m**, IC_{50}: 56 nM), di-methylamine (**5n**, IC_{50}: 66 nM) and *N*-acetyl derivative (**5o**: IC_{50}: 89 nM) displayed comparatively weaker JAK3 inhibitory activity.

In Set-1, compound **5k** (methane sulfonate) showed potent JAK3 inhibitory activity, which was found to be comparable to the Cerdulatinib (IC_{50}: 8 nM; Table 1) and 5 fold less potent compared to Tofacitinib (IC_{50}: 1.6 nM). Thus, in the Set-1, substitution on *p*-position of phenyl ring, followed by replacement of *N*-acetyl to *O*-sulfonate led to the single digit nM potent compound (**5k**), with moderate isoform selectivity (Table 3).

Further, to improve JAK3 isoform selectivity, modifications were carried out in the **5k**. In the second set (Table 2), variations were carried out at the C4-position of pyrimidine, in **5k**. As listed in the Table 2 (compounds **11a-o**), compound **11a (**debenzylated **5k**; IC_{50}: 300 nM) was found to be less active. Replacement of benzyl group with cycloalkyl groups, compound **11b** (cyclopropyl, IC_{50}: 49 nM), **11c** (cyclobutyl, IC_{50}: 37 nM), **11d** (cyclopentyl, IC_{50}: 33 nM) and **11e** (cyclohexyl, IC_{50}: 79 nM) showed moderate activities. Overall, the cycloalkyl derivatives were found to be less potent compared to **5k**. Compound **11f** (pyran, IC_{50}: 12 nM) showed slight improvement in the activity, while **11g** (iso-butane, IC_{50}: 9.8 nM) was found to be equipotent as the **5k**. Racemic compound **11h** (iso-pentane, IC_{50}: 20 nM) showed two fold less potency compared to **5k**. Chirally pure compound **11i** (R-isomer of **11h**) was found to be five-fold more potent (IC_{50}: 1.7 nM), whereas **11j** (S-isomer of **11h**) was found to be least potent (IC_{50}: 256 nM). Compound **11k** (phenyl ethyl, IC_{50}: 39 nM), fluoro-substituted benzyl analogues, **11l** (3-fluoro), **11m** (4-fluoro) and **11n** (2-fluoro) showed moderate activities (IC_{50} >40 nM) compared to **5k**, while **11o** (naphthyl, IC_{50}: 189 nM) was found to be less active.

2.4. JAKs Isoform Selectivity (enzyme based biochemical screening):

Most potent compounds (**5k** and **11i**) were evaluated for their selectivity against JAK isoforms (JAK-1, 2 and TYK2). [32] As shown in Table 3, initial hit (**5k**) showed moderate selectivity (2 to 5X) against JAK isoforms over JAK3. Compound **11i** (IC_{50}: 1.7 nM) demonstrated 12, 100, and 109 fold selectivity over JAK1, JAK2 and TYK2 respectively. Selectivity profile of **11i** against all the three isoforms was found to be better than standard compounds. Thus, potency and selectivity of diaminopyrimidine-5-carboxamides based JAK3 inhibitors can be modulated using suitable substituents at C2 and C4-position of pyrimidine ring.

*2.5. Profiling of **11i** (in vitro and ex vivo):*

In vitro kinase profiling study of compound **11i** was carried out at 1μM concentration, against Millipore panel of 170 purified kinases (n=2) and the % inhibition was found to be < 20% at 1μM concentration, including key cysteine containing protein kinases (TEC family (BMX, BTK, ITK, TXK, and TEC), ErbB family (EGFR, ERBB4, and ERBB2), CLK2, MKK7β, PKG1α and Aurora kinase), see Table 8.

JAK3 selectivity of **11i** was evaluated under physiologic conditions (cellular assay) to understand role of the associated cytokine receptors and downstream inflammatory pathways inhibited. To elucidate potency and selectivity profile in a cellular environment, compound **11i** was tested for the inhibition of phosphorylation of downstream signal (STAT proteins), in the human peripheral blood mononuclear cells (PBMCs) [33]. The different cellular stimuli were used to induce phosphorylation of STATs (pSTAT), either by dual JAK1/3 (IL-2 stimulus, pSTAT5), JAK2 (GM-CSF stimulus, pSTAT5), or with the PAN JAK1/JAK2/TYK2 (IL-6 stimulus, pSTAT3) stimuli [34]. As shown in Table 4, **11i** showed 27-fold selectivity for inhibition of the IL-2 (IC_{50}: 22.16 nM) versus the IL-6 readout (IC_{50}: 608 nM) and a 23-fold selectivity for the inhibition of the GM-CSF (IC_{50}: 511 nM). Tofacitinib displayed similar potencies but lower selectivity than **11i** in the relevant pSTAT assays. Thus, compound **11i** showed preferential inhibition of JAK3 over JAK1, in the JAK/STAT signaling pathway, when assessed in the PBMC assay.

Ex vivo, compound **11i** was evaluated for the plasma protein binding studies (using mice, rat and human plasma) and liver microsomal stability studies (using immortalized mice, rats and human liver cell line). Compound **11i** showed 75 to 80% plasma protein binding and less than 10% metabolism at 30 minutes, in microsomal metabolic stability study. Compound **11i** was found to be devoid of CYP (<10% CYP inhibition) at 10 μM concentration, for CYP1A2, CYP2C8, CYP2C9, CYP2D6, CYP2C19 and CYP3A4 and hERG liabilities (IC_{50}: > 10 μM).

2.6. Pharmacokinetic study:

In a single dose PK studies (3 mg/kg, po and 1 mg/kg, iv, in male C57BL/6J mice) of compounds **5k**, **11i** and Tofacitinib, various PK parameters (Tmax, Cmax, $t_{1/2}$, Cl, AUC and %F) were recorded (Table 5). Compound **5k** showed moderate AUC, due to its high clearance, which resulted into overall low bioavailability (15%). Compound **11i** showed higher AUC (~10 fold, compared to std), extended $t_{1/2}$ (2.56 hr) and good oral bioavailability (%F: ~48 over std, 20%). Compound **11i** showed extended $t_{1/2}$ and higher AUC, which could be due to its low clearance compared to standard (11.59 vs 47.56 ml/min/kg, iv).

2.7. In vivo efficacy studies:

2.7.1 Anti-arthritic efficacy of test compounds in Collagen Induced Arthritis (CIA) mice model:

Arthritis was developed in male DBA1j mice, using collagen mixture and mice were recruited for the study once clinical signs were visible. [35] Considering low bioavailability of **5k**, only **11i** was evaluated. Eight animals were assigned in each of the three groups [vehicle, positive control (Tofacitinib, 60 mg/kg) and test compound **11i** (30 mg/kg)]. Treatment was continued for three weeks and percentage inhibition in clinical score was recorded.

As shown in the Fig.2a, standard compound and **11i** showed good reduction in the arthritic score, compared to vehicle control (untreated group). Two fold higher dose of a standard compound was used, considering >2X difference in the mice oral bioavailability. At 30 mg/kg dose, compound **11i** showed comparable anti-arthritic activity to that of standard compound (dose 60 mg/kg). Body weights of the animals were also recorded 3 times a week as a measure of treatment related side effect. No changes in the mice body weight was observed in any treatment group, compared to vehicle control group. Thus improved PK of **11i** justifies its potent *in vivo* efficacy in the CIA mice model.

2.7.2 Anti-arthritic efficacy of test compounds in AIA (Adjuvant induced Arthritis) rat model:

Anti-arthritic efficacy of the compound **11i** was evaluated in a rat AIA model.[36] As shown in the Fig.2b, standard and **11i** showed good reduction in the paw volume, compared to vehicle control (untreated group). Compound **11i** suppressed paw swelling in a dose-dependent manner (ED_{50}: 10 mg/kg) and at 30 mg/kg dose, efficacy of **11i** was found to be comparable to that of standard (Tofacitinib, 60 mg/kg). Body weight was not significantly affected in rats, in any treatment group compared to the vehicle control group.

2.8 Safety pharmacology:

To assess the safety profile of compound **11i**, repeat dose acute toxicity studies (14 days) was carried out in male Wistar rats (100 mg/kg, po, once daily) and various parameters such as gross pathology, clinical signs, body weight, organ weight and serum chemistry/hematological changes were recorded. Daily oral administration of compounds **11i** (10X of ED_{50} dose), over a period of 2 weeks did not affect the survival of Wistar rats and also no adverse changes related to gross pathology, clinical signs, body weight and feed consumption were noticed, compared to control group. As shown in Table 6 and 7, the hematological parameters (WBC and RBC) of compounds **11i** were found to be comparable to that of control animals. Similarly, compound **11i** showed no significant changes in serum hepatotoxicity assessment parameters as compared to the control group. Also compound **11i** treated groups showed no changes in the key organs (heart, kidney, spleen and brain) weights.

2.9. Docking study:

In the docking studies, Cerdulatinib binds in a similar orientation to that of 4,6-diaminonicotinamide of the co-crystallized ligand (9YV; 4-(benzylamino)-6-({4-[(1-methylpiperidin-4-yl)carbamoyl]phenyl}amino)pyridine-3-carboxamide), maintaining hydrogen bonding interactions with the hinge region of JAK3 (a ‘classical’ triad hinge binding interaction), Fig.3. The docked poses of the core of Cerdulatinib and the co-crystallized ligand superimposed well. Compound **11i** showed similar interactions as that of Cerdulatinib, in the hinge region and superimposed very well with the core of Cerdulatinib. However, **11i** showed additional interaction with the Cys909 (hydrogen bond between NH of Cys909 with oxygen of methyl sulfonate group), which was not observed with the Cerdulatinib. An additional interactions of **11i** with the Cys909, in the catalytic domain of JAK3 enzyme likely to contribute towards its potent and selective JAK3 inhibitory activity. The docking score for Cerdulatinib and **11i** was found to be -8.6 and -9.9 kcal mol^{-1} respectively.

3. Conclusion

In summary, we have described discovery and characterization of a novel JAK3 inhibitor, compound **11i**. Two series of 2,4-diaminopyrimidine-5-carboxamide derivatives were evaluated as a JAK3 inhibitors. Modifications at the C2-position of pyrimidine ring led to an identification of a single digit nM potent JAK3 inhibitor (**5k**), with moderate isoform selectivity. Further structure-activity relationship (SAR) studies on the C4-position of **5k** resulted in to the discovery of (R)-4-((5-carbamoyl-4-((3-methylbutan-2-yl)amino)pyrimidin-2-yl)amino)phenyl methane sulfonate (**11i**) that showed improved isoform selectivity in the biochemical assay. Compound **11i** selectively inhibits JAK3 cytokine signaling in the primary cells, which translated to the promising efficacy in animal models of RA. In the repeat dose acute toxicity study, **11i** showed no adverse changes related to gross pathology, clinical signs and liver toxicity, indicating that the new class JAK3 selective inhibitor could be viable therapeutic option for the treatment of rheumatoid arthritis.

4. Experimental section

4.1 Materials and methods:

NMR spectra were measured on a Varian Unity 400 (^{1}H at 400 MHz, ^{13}C at 100 MHz), magnetic resonance spectrometer. Spectra were taken in the indicated solvent at ambient temperature. Chemical shifts (δ) are given in parts per million (ppm) with tetramethylsilane as an internal standard. Multiplicities are recorded as follows: s = singlet, d = doublet, t = triplet, q = quartet, br = broad, m = multiplet. Coupling constants (*J* values) are given in Hz. Mass spectra are recorded on Perkin-Elmer Sciex API 3000. Reactions were monitored using thin layer silica gel chromatography (TLC) using 0.25 mm silica gel 60F plates from Merck. Plates were visualized by treatment with UV, acidic p-anisaldehyde stain, $KMnO_4$ stain with gentle heating. Products were purified by column chromatography using silica gel 100-200 mesh and the solvent systems indicated.

4.2 General synthesis:

*4.2.1. 4-(Benzylamino)-2-(methylthio)pyrimidine-5-carboxylic acid **(2)***

Ethyl 4-chloro-2-(methylthio)pyrimidine 5-carboxylate **(1)** 13.3 g (57.2 mmol) dissolved in dioxane 100 mL and DIPEA 10.99 mL (62.9 mmol) was added to the reaction mixture at 0°C, followed by addition of benzyl amine 6.13 g (57.2 mmol) and the reaction mixture was stirred at 0°C for 30 min, and then 6 h. at RT. LiOH 6.85 g (286 mmol) was dissolved in 50 mL water and added in to reaction mixture and stirred overnight at 28°C. After completion of reaction, the reaction mixture was concentrated by rotary evaporation to remove a majority of the dioxane, and then acidified with 10 M HC1 to pH ~ 5, resulting in the formation of a white precipitate. The solid compound was filtered, washed with water and dried under vacuum to afford the 4-(benzylamino)-2 (methylthio) pyrimidine-5-carboxylic acid **(2)** as white solid. (13.23 g, 84 %). ^{1}H NMR (DMSO-d_6, 400 MHz) δ ppm: 2.59 (s, 3H), 4.69 (d, *J = 6.0 Hz*, 3H), 7.28 - 7.22 (m ,1H), 7.30 - 7.33 (m, 4H), 8.52.(s, 1H), 9.25 (s, 1H). ESI-MS: m/z Calcd for $C_{13}H_{14}N_3O_2S$ $[M+1]^+$ 276.33, found 276.05.

*4.2.2. 4-(Benzylamino)-2-(methylthio)pyrimidine-5-carboxamide **(3).***

4-(Benzylamino)-2-(methylthio)pyrimidine-5-carboxylic acid **(2)** 12 g (43.6 mmol) was dissolved in DMF 100 mL, under nitrogen atmosphere and treated with HOBT 6.68 g (43.6 mmol) and EDC.HCI 16.68 g (87.0 mmol) at RT. After stirring 1 hr., aq. Ammonia (40 mL) was added at 0° C, and it was stirred further for 1 h., at RT. Reaction mixture was quenched by ice - water (200 mL), resulted in the formation of a white precipitate. The solid compound was filtered, washed with water and dried under to afford 4-(benzylamino)-2-(methylthio)pyrimidine-5-carboxamide **(3)** (11.36 g, 95 %). ^{1}H NMR (DMSO-d_6, 400 MHz) δ ppm: 2.40 (s, 3H), 4.67 (d, *J = 6.0 Hz*, 2H), 7.23 - 7.28 (m, 1H), 7.31- 7.35 (m, 4H), 7.45 (s, 1H), 8.04 (s, 1H), 8.53 (s, 1H), 9.48 (t, *J* = 6.0 Hz,1H). ESI-MS : m/z Calcd for $C_{13}H_{15}N_4OS$ $[M+1]^+$ 275.34, found 275.08.

*4.2.3. 4-(Benzylamino)-2-(methylsulfinyl)pyrimidine-5-carboxamide **(4).***

4-(Benzylamino)-2-(methylthio)pyrimidine-5-carboxamide (**3**; 11 g (40.1 mmol)) was dissolved in a mixture of dioxane and chloroform (1:1; 290 mL). Reaction mixture was cooled up to -2°C and treated with m-CPBA (60%; 17.3 g, 60.1 mmol) and it was stirred for 50 min at 0°C. Reaction mixture was quenched with 10% aq. sodium metabisulfite (290mL) and extracted with chloroform. Organic layer was washed with aq. 10 % sodium bicarbonate. The organic layer was dried over sodium sulfate (42 g) and the solvent was removed under reduced pressure to afford 4-(benzylamino)-2-(methylsulfinyl)pyrimidine-5-carboxamide **(4)** as white solid. (9.31 g, 80 %). ^{1}H NMR (DMSO-d$_6$, 400 MHz) δ ppm 2.75 (s, 3H), 4.70 (d, *J = 6.0 Hz*, 2H), 7.24 - 7.31 (m, 1H), 7.33 - 7.38 (s, 4H), 7.74 (s, 1H), 8.28 (s, 1H), 8.76 (s, 1H), 9.60 (t, *J = 5.6 Hz*, 2H). ESI-MS : m/z Calcd for $C_{13}H_{15}N_4O_2S$ $[M+1]^+$ 291.34, found 291.00.

4.2.4. General procedure for the synthesis of compound ***5a-o.***

To a solution of 4-(benzylamino)-2-(methylsulfinyl)pyrimidine-5-carboxamide (**4**; 1.0 eq) and PTSA (1.1 eq)), in NMP was added different substituted aryl amines (1.0 eq), at RT. The reaction mixture was heated at 100-110°C for 1-2 h. After completion of reaction, the mixture was diluted with water and the compound was extracted in EtOAc. Organic layer was dried over sodium sulfate, filtered and concentrated under vacuum to afford the crude product. Crude product was purified by flash chromatography over silica gel (100-200 mesh) with 2 % MeOH/$CHCl_3$ to provide the desired title product **5a-o**.

4*.2.4.1. 2-((3-Aminophenyl)amino)-4-(benzylamino)pyrimidine-5-carboxamide* ***(5a)***. Refer to general procedure for the synthesis of **5a**, as described in section 4.1.4. 51.2% isolated yield; white solid. ^{1}H NMR (DMSO-d$_6$, 400 MHz) δ ppm 4.67 (d, *J = 5.6 Hz*, 2H), 6.18 (d, J = 6.8 Hz, 1H), 6.82-6.86 (m, 2H), 6.97 (s, 1H), 7.22 - 7.35 (m, 5H), 8.51 (s, 1H), 9.20 (s, 1H), 9.47 (t, *J = 6 Hz*, 1H). ^{13}C NMR (DMSO-d6, 100 MHz) δ ppm 43.9, 100.5, 100.9, 103.2, 107.0, 126.6, 127.0, 128.7, 129.5, 139.9, 142.9, 148.0, 161.8, 165.1, 166.2, 169.6. ESI-MS : m/z Calcd for $C_{18}H_{19}N_6O$ $[M+1]^+$ 335.38, found 334.90.

4.2.4.2. Methyl-2-((3-((4-(Benzylamino)-5-carbamoylpyrimidin-2-yl)amino)phenyl)amino)-2-oxoacetate ***(5b)***. Refer to general procedure for the synthesis of **5b**, as described in section 4.1.4. 49.5% isolated yield; white solid. ^{1}H NMR (DMSO-d$_6$, 400 MHz) δ ppm 3.84 (s, 3H), 4.72 (d, *J = 6.0 Hz*, 2H), 7.18 - 7.31 (m, 8H), 8.25 (s, 1H), 8.55 (s, 1H), 9.71 (s, 2H), 10.68 (s, 1H). ^{13}C NMR (DMSO-d6, 100 MHz) δ ppm 43.8, 51.1, 100.4, 107.8, 111.0, 113.6, 126.5, 127.1, 128.8, 129.6, 137.2, 140.0, 142.7, 155.0, 162.2, 164.5, 165.9, 166.8, 169.7. ESI-MS: m/z Calcd for $C_{21}H_{21}N_6O_4$ $[M]^+$ 420.43, found 420.80.

4.2.4.3. 2-((3-((4-(Benzylamino)-5-carbamoylpyrimidin-2-yl)amino)phenyl)amino)-2-oxoacetic acid ***(5c)***. Refer to general procedure for the synthesis of **5c**, as described in section 4.1.4. 51.9% isolated yield; white solid. ^{1}H NMR (DMSO-d$_6$, 400 MHz) δ ppm 4.71 (d, *J = 6.0 Hz*, 2H), 6.98 - 7.70 (m, 7H), 7.86 - 7.94 (m, 1H), 8.17 (s, 1H), 8.53 (s, 1H), 9.62 (s, 2H), 10.58 (s, 1H). ^{13}C NMR (DMSO-d6, 100 MHz) δ ppm 43.8, 100.5, 107.9, 110.9, 113.8, 126.5, 127.1, 128.8, 129.9, 137.8, 140.1, 143.0, 156.9, 162.0, 164.1, 166.0, 166.9, 169.5. ESI-MS: m/z Calcd for $C_{20}H_{18}N_6O_4$ $[M]^+$ 406.40, found 406.02.

4.2.4.4. 4-(Benzylamino)-2-((3-cinnamamidophenyl)amino)pyrimidine-5-carboxamide ***(5d)***. Refer to general procedure for the synthesis of **5d**, as described in section 4.1.4. 48.8% isolated yield; white solid. ^{1}H NMR (DMSO-d$_6$, 400 MHz) δ ppm 4.74 (d, *J = 6.0 Hz*, 2H), 6.84 (s, 1H), 6.88 (s, 1H), 7.21 - 7.32 (m, 5H), 7.38 - 7.45 (m, 5H), 7.47 - 7.61 (m, 3H), 8.14 (s, 1H), 8.56 (s, 1H), 9.53 (s, 2H), 10.11 (s, 1H). ^{13}C NMR (DMSO-d6, 100 MHz) δ ppm 43.5, 100.4, 108.0, 111.2, 113.9, 119.0, 126.7, 127.4, 128.0, 128.4, 128.7, 128.9, 129.6, 135.6, 137.1, 139.8, 142.0, 143.2, 162.2, 165.8, 166.7, 167.2, 169.8. ESI-MS: m/z Calcd for $C_{27}H_{25}N_6O_2$ $[M]^+$ 464.53, found 464.90.

4.2.4.5. 4-(benzylamino)-2-((3-(methylsulfonamido)phenyl)amino)pyrimidine-5carboxamide ***(5e)***. Refer to general procedure for the synthesis of **5e**, as described in section 4.1.4. 50.8% isolated yield; white solid.^{1}H NMR (DMSO-d$_6$, 400 MHz) δ ppm 3.33 (s, 3H), 4.70 (d, *J = 5.6 Hz*, 2H), 7.10 - 7.05 (m ,2H), 7.31 - 7.35 (m, 4H), 7.80 - 7.88 (m, 2H), 7.94 (s, 1H), 8.59 (s, 1H), 9.55 (s, 1H), 9.69 (s, 1H). ^{13}C NMR (DMSO-d6, 100 MHz) δ ppm 40.0, 44.5, 101.0, 101.5, 107.4, 109.0, 126.5, 127.1, 128.6, 130.0, 138.3, 139.5, 143.0, 161.9, 165.5, 167.0, 169.1. ESI-MS: m/z Calcd for $C_{19}H_{20}N_6O_3S$ $[M]^+$ 412.47, found 412.22.

4.2.4.5. 4-(Benzylamino)-2-((3-(S-methylsulfonimidoyl)phenyl)amino)pyrimidine-5-carboxamide ***(5f)***. Refer to general procedure for the synthesis of **5f**, as described in section 4.1.4. 45.9% isolated yield; white solid. ^{1}H NMR (DMSO-d$_6$, 400 MHz) δ ppm 2.51 (s, 3H), 4.65 (d, *J = 6.0 Hz*, 2H), 6.80 - 6.87 (m ,2H), 7.26 - 7.27 (m, 5H), 7.33 - 7.34 (m, 2H), 8.37 (s, 1H), 9.61 (s, 1H), 9.78 (s, 1H). ^{13}C NMR (DMSO-d6, 100 MHz) δ ppm 43.8, 44.2, 100.9, 112.2, 114.5, 120.3, 126.8, 127.0, 128.7, 128.9, 140.1, 142.3, 146.8, 162.0, 165.9, 168.2, 169.8. ESI-MS: m/z Calcd for $C_{19}H_{20}N_6O_2S$ $[M]^+$ 396.47, found 396.20

*4.2.4.6. 4-(Benzylamino)-2-((3-(N-(methylsulfonyl)acetamido)phenyl)amino)pyrimidine-5 carboxamide **(5g)***. Refer to general procedure for the synthesis of **5g**, as described in section 4.1.4. 49.6% isolated yield; white solid. ^{1}H NMR (DMSO-d$_6$, 400 MHz) δ ppm 1.83 (s, 3H), 3.46 (s, 3H), 4.70 (d, *J = 6.0 Hz*, 2H), 7.03 (d, *J = 7.2 Hz*, 1H), 7.23 - 7.26 (m, 1H), 7.31 - 7.35 (m, 5H), 7.66 (d, *J = 7.2 Hz*, 1H), 7.93 (S, 1H), 8.59 (s, 1H), 9.64 (s, 1H), 9.75 (s, 1H). ^{13}C NMR (DMSO-d6, 100 MHz) δ ppm 20.0, 43.7, 44.0, 101.2, 108.4, 113.9, 119.9, 126.9, 127.2, 128.6, 129.1, 131.5, 140.0, 142.5, 162.3, 166.2, 166.5, 168.5, 169.7. ESI-MS: m/z Calcd for $C_{21}H_{23}N_6O_4S$ $[M+1]^+$ 455.50, found 455.00.

*4.2.4.7. 4-(Benzylamino)-2-((4-(methylsulfonamido)phenyl)amino)pyrimidine-5-carboxamide **(5h)***. Refer to general procedure for the synthesis of **5h**, as described in section 4.1.4. 47.8% isolated yield; white solid. ^{1}H NMR (DMSO-d$_6$, 400 MHz) δ ppm 2.90 (s, 3H), 4.67 (d, *J = 6.0 Hz*, 2H), 7.05 (d, *J = 9.2 Hz*, 2H), 7.32 - 7.33 (m, 5H), 7.58 (d, *J = 8.8 Hz*, 2H), 8.54 (s, 1H), 9.39 (s, 1H), 9.45 (s, 1H), 9.47 (s, 1H). ^{13}C NMR (DMSO-d6, 100 MHz) δ ppm 43.9, 43.6, 100.8, 117.9, 118.6, 126.6, 126.9, 127.8, 128.2, 128.9, 139.8, 162.5, 166.2, 168.5, 169.8. ESI-MS: m/z Calcd for $C_{19}H_{20}N_6O_3S$ $[M]^+$ 412.47, found 412.80.

*4.2.4.8. 4-(Benzylamino)-2-((4-(S-methylsulfonimidoyl)phenyl)amino)pyrimidine-5-carboxamide **(5i)***. Refer to general procedure for the synthesis of **5i**, as described in section 4.1.4. 45.2% isolated yield; white solid. ^{1}H NMR (DMSO-d$_6$, 400 MHz) δ ppm 2.50 (s, 3H) 4.41 (d, *J = 6.0 Hz*, 2H), 6.64 (d, *J = 8.8 Hz*, 2H), 7.22 - 7.32 (m, 5H), 7.54 (d, *J = 8.0 Hz*, 2H), 8.45 (s, 1H), 9.42 (s, 1H), 9.65 (s, 1H). ^{13}C NMR (DMSO-d6, 100 MHz) δ ppm 43.8, 45.2, 101.7, 115.0, 126.2, 126.5, 126.7, 128.0, 136.2, 140.0, 141.3, 162.4, 166.1, 168.8, 169.5. ESI-MS: m/z Calcd for $C_{19}H_{20}N_6O_2S$ $[M]^+$ 396.47, found 396.80.

*4.2.4.9. 4-(Benzylamino)-2-((4-(N-(methylsulfonyl)acetamido)phenyl)amino)pyrimidine-5-carboxamide **(5j)***. Refer to general procedure for the synthesis of **5j**, as described in section 4.1.4. 49.7% isolated yield; white solid.^{1}H NMR (DMSO-d$_6$, 400 MHz) δ ppm 1.88 (s, 3H), 3.49 (s, 3H), 4.70 (d, *J = 6.0 Hz*, 2H), 7.22 - 7.31 (m, 5H), 7.33 - 7.36 (m, 2H), 7.78 (d, *J = 8.8 Hz*, 2H), 8.58 (s, 1H), 9.57 (t, *J = 6.0 Hz*, 1H), 9.74 (s, 1H).). ^{13}C NMR (DMSO-d6, 100 MHz) δ ppm 19.5, 42.9, 43.7, 100.5, 117.6, 119.6, 121.8, 126.4, 126.9, 127.9, 139.7, 140.1, 162.8, 166.9, 167.2, 168.8, 169.2. ESI-MS m/z Calcd for $C_{21}H_{23}N_6O_4S$ $[M]^+$ 454.50, found 454.90.

4.2.4.10. 4-((4-(Benzylamino)-5-carbamoylpyrimidin-2-yl)amino)phenyl methanesulfonate ***(5k)***. Refer to general procedure for the synthesis of **5k**, as described in section 4.1.4. 51.5% isolated yield; white solid. ^{1}H NMR (DMSO-d$_6$, 400 MHz) δ ppm 3.33 (s, 3H) 4.68 (d, *J = 5.6 Hz*, 2H), 7.18 (d, *J = 8.4 Hz*, 2H), 7.22 - 7.35 (m, 5H), 7.73 (d, *J = 8.4 Hz*, 2H), 8.56 (s, 1H), 9.57 (s, 1H), 9.66 (s, 1H). ^{13}C NMR (DMSO-d6, 100 MHz) δ ppm 37.5, 44.0, 100.5, 120.5, 122.6, 127.4, 127.8, 128.9, 139.8, 143.5, 157.7, 160.2, 161.9, 169.4. ESI-MS: m/z Calcd for $C_{19}H_{20}N_5O_4S$ $[M]^+$ 413.45, found 413.90.

4.2.4.11. 4-((4-(Benzylamino)-5-carbamoylpyrimidin-2-yl)amino)phenyl propane-2-sulfonate ***(5l)***. Refer to general procedure for the synthesis of **5l**, as described in section 4.1.4. 50.5% isolated yield; white solid. ^{1}H NMR (DMSO-d$_6$, 400 MHz) δ ppm 1.41 (d, *J = 6.8 Hz*, 6H), 3.64 - 3.67 (m, 1H), 4.68 (d, *J = 6.0 Hz*, 2H), 7.13 (d, *J = 9.2 Hz*, 2H), 7.23 - 7.34 (m, 5H), 7.71 (d, *J = 9.2 Hz,* 2H), 8.56 (s, 1H), 9.55 (s, 1H), 9.65 (s, 1H). ^{13}C NMR (DMSO-d6, 100 MHz) δ ppm 16.0, 43.8, 49.8, 100.7, 121.0, 122.4, 127.3, 127.7, 128.6, 138.9, 142.9, 158.0, 160.9, 162.2, 169.8. ESI-MS: m/z Calcd for $C_{21}H_{24}N_5O_4S$ $[M+1]^+$ 442.51, found 442.10.

4.2.4.12. 2-Amino-4-((4-(benzylamino)-5-carbamoylpyrimidiyl) amino) phenyl methane sulfonate ***(5m)***. Refer to general procedure for the synthesis of **5m**, as described in section 4.1.4. 49.8% isolated yield; white solid. ^{1}H NMR (DMSO-d$_6$, 400 MHz) δ ppm 3.33 (s, 3H) 4.68 (d, *J = 6.0 Hz*, 2H), 5.18 (s, 2H), 6.88 - 6.95 (m, 2H), 7.19 - 7.26 (m, 2H), 7.30 - 7.36 (m, 4H), 8.53 (s, 1H), 9.37 (s, 1H), 9.49 (t, *J = 5.8 Hz*, 2H). ^{13}C NMR (DMSO-d6, 100 MHz) δ ppm 37.9, 44.0, 100.1, 107.1, 108.1, 123.2, 127.3, 127.7, 128.8, 130.7, 139.9, 140.0, 141.1, 157.7, 160.4, 161.9, 169.5. ESI-MS: m/z Calcd for $C_{19}H_{21}N_6O_4S$ $[M+1]^+$ 429.47, found 429.00.

4.2.4.13. 4-((4-(Benzylamino)-5-carbamoylpyrimidin-2-yl)amino)-2-(dimethylamino)phenyl methane sulfonate ***(5n)***. Refer to general procedure for the synthesis of **5n**, as described in section 4.1.4. 46.8% isolated yield; white solid. ^{1}H NMR (DMSO-d$_6$, 400 MHz) δ ppm 2.67 (s, 6H), 3.32 (s, 3H), 4.72 (d, *J = 5.6 Hz*, 2H), 7.05 (d, *J = 8.8 Hz*, 1H), 7.23 - 7.29 (m, 2H), 7.33 - 7.36 (m, 4H), 7.57 (s, 1H), 8.57 (s, 1H), 9.55 (s, 2H). ^{13}C NMR (DMSO-d6, 100 MHz) δ ppm 37.4, 42.9, 44.2, 100.9, 107.7, 108.4, 127.1, 127.9, 128.5, 130.4, 140.0, 140.2, 143.8, 157.3, 160.7, 161.4, 169.2. ESI-MS: m/z Calcd for $C_{21}H_{25}N_6O_4S$ 456.52 $[M]^+$, found 456.90.

4.2.4.14. 4-((4-(Benzylamino)-5-carbamoylpyrimidin-2-yl)amino)-2-carbamoylphenyl methane sulfonate ***(5o)***. Refer to general procedure for the synthesis of **5o**, as described in section 4.1.4.

48.5% isolated yield; white solid. ^{1}H NMR (DMSO-d_6, 400 MHz) δ ppm 2.05 (s, 3H), 3.33 (s, 3H), 4.71 (d, *J = 6.0 Hz*, 2H), 7.26 - 7.19 (m, 6H), 7.47 (d, *J = 7.6Hz*, 1H), 8.31 (s, 1H), 8.57 (s, 1H), 9.50 (s, 1H), 9.54 (s, 1H), 9.67(s, 1H). ^{13}C NMR (DMSO-d6, 100 MHz) δ ppm 23.8, 38.1, 43.9, 100.7, 109.1, 116.2, 123.1, 127.2, 127.5, 128.8, 131.2, 139.6, 139.8, 142.0, 157.7, 160.3, 161.9, 163.2, 169.4. ESI-MS: m/z Calcd for $C_{21}H_{23}N_6O_5S$ $[M+1]^+$ 471.50, found 471.19.

*4.2.5. Preparation of Ethyl 4-hydroxy-2-((4-((methylsulfonyl)oxy) phenyl)amino) pyrimidine -5-carboxylate **(7)***

Ethyl 4-hydroxy-2-(methylthio)pyrimidine-5-carboxylate (**6**; 10 g; 46.7 mmol) was dissolved in a mixture of dioxan and chloroform (1:1; 262 mL). Reaction mixture was cooled up to -2°C, treated with m-CPBA (60%; 20.14 g, 70.0 mmol) and stirred for 50 min at 0°C. Reaction mixture was quenched by 10% aq. sodium metabisulfite (262 mL), extracted with chloroform and washed with aq. 10 % sodium bicarbonate. The organic layer was dried over sodium sulfate (40 g) and the solvent was evaporated under reduced pressure to obtain ethyl 4-hydroxy-2-(methylsulfinyl)pyrimidine-5-carboxylate as a white solid. (8.6 g, 80 %), which was further used in the next step without purification.

To the mixture of ethyl 4-hydroxy-2-(methylsulfinyl)pyrimidine-5-carboxylate (8.6 g; 37.4 mmol) and PTSA (7.82 g; 41.1 mmol), dissolved in NMP (80ml) was added 4-(methylsulfonyl)aniline (6.99 g; 37.4 mmol), at RT. The reaction mixture was heated at 100-110°C for 1-2 h. After completion of reaction, the mixture was diluted with water and the compound was extracted in EtOAc. Organic layer was dried over sodium sulfate, filtered and concentrated under vacuum to afford the crude product. Crude product was purified by flash chromatography over silica gel (100-200 mesh) with 2 % MeOH/$CHCl_3$ to get the ethyl 4-hydroxy-2-((4-((methylsulfonyl) oxy)phenyl)amino) pyrimidine-5-carboxylate **(7)** (9.9 g, 75%). ^{1}H NMR (DMSO-d_6, 400 MHz) δ ppm 1.26 (t, *J = 7.0 Hz*, 3H), 3.48 (s, 3H), 4.20 (q, *J = 6.8 Hz*, 2H), 6.57 (d, *J = 9.2 Hz*, 2H), 7.34 (d, *J = 8.8 Hz*, 2H), 8.49 (s, 1H), 9.75 (s, 1H), 11.25 (s, 1H): ESI-MS: m/z Calcd for $C_{14}H_{16}N_3O_6S$ $[M+1]^+$ 354.35, found 354.58.

*4.2.6. 4-hydroxy-2-((4-((methylsulfonyl)oxy)phenyl)amino)pyrimidine-5-carboxylic acid **(8).***

Ethyl 4-hydroxy-2-((4-((methylsulfonyl)oxy)phenyl)amino)pyrimidine-5-carboxylate (**7**; 9.0 g, 25.5 mmol) was dissolved in THF (90mL). LiOH (3.05 g, 127 mmol) dissolved in water (5mL) was added in to the reaction mixture and stirred overnight at 25°C. After completion of reaction, the reaction mixture was concentrated by rotary evaporation to remove excess THF. Mixture was acidified (10 M HC1 to pH ~ 5), which led to the formation of a white precipitate. The solid compound filtered, washed with water and dried under vacuum to afford 4-hydroxy-2-((4-((methylsulfonyl)oxy)phenyl)amino)pyrimidine-5-carboxylic acid **(8),** as a white solid. (6.63 g, 80%). 1H NMR (DMSO-d6, 400 MHz) δ ppm 3.56 (s, 3H), 7.37 (d, J = 8.8 Hz, 2H), 7.67 (d, *J* = 8.8 Hz, 2H), 8.51 (s, 1H), 9.85 (s, 1H). ESI-MS: m/z Calcd for $C_{12}H_{12}N_3O_6S$ $[M+1]^+$ 326.30, found 326.01.

4.2.7. 4-((5-carbamoyl-4-hydroxypyrimidin-2-yl)amino)phenyl methanesulfonate ***(9).***

4-Hydroxy-2-((4-((methylsulfonyl)oxy)phenyl)amino)pyrimidine-5-carboxylic acid (**8**; 6.0 g, 18.44 mmol) was dissolved in DMF (50 mL) and treated with HOBT (2.82 g; 18.44 mmol) and EDC.HCI (7.07 g; 36.9 mmol), at RT. After stirring 1 hr., aq. Ammonia (20 mL) was added at 0°C and stirred for 1 hr., at RT. The reaction mixture was quenched with water (200 mL) which resulted in the formation of a white precipitate. The solid compound was filtered, washed with water and dried under reduced pressure to afford 4-((5-carbamoyl-4-hydroxypyrimidin-2-yl)amino)phenyl methanesulfonate (**9**; 4.19 g, 70%). ^1H NMR (DMSO-d_6, 400 MHz) δ ppm 3.33 (s, 3H), 7.21 (d, *J = 8.8 Hz*, 2H), 7.87 (d, *J = 8.8 Hz*, 2H), 8.37 (s, 1H), 9.33 (s, 1H), 17.6 (s, 1H). ESI-MS: m/z Calcd for $C_{12}H_{13}N_4O_5S$ $[M+2]^+$ 324.31, found 326.05.

4.2.8. 4-((5-carbamoyl-4-chloropyrimidin-2-yl)amino)phenyl methanesulfonate ***(10).***

To a solution of 4-((5-carbamoyl-4-hydroxypyrimidin-2-yl)amino)phenyl methanesulfonate (**9**; 4.0 g,12.33 mmol), in toluene (50 mL) was added DIPEA (2.6 mL, 14.8 mmol) and $POCl_3$ (2.3 mL, 24.67 mmol) drop wise, at 0-5^{o}C. The reaction mixture was refluxed for 2 hr. After completion of reaction, mixture was cooled to RT, quenched with ice - water (180 mL) to afford white precipitate. The precipitated compound was filtered, washed with cold water to get 4-((5-carbamoyl-4-chloropyrimidin-2-yl)amino)phenyl methanesulfonate (**10**; 2.96 g, 70%). ^1H NMR (DMSO-d_6, 400 MHz) δ ppm 3.37 (s, 3H), 7.34 (d, *J = 9.2 Hz*, 2H), 7.80 (d, *J = 9.2 Hz*, 2H), 8.92 (s, 1H), 10.70 (s, 1H). ESI-MS: m/z Calcd for $C_{12}H_{12}ClN_4O_4S$ $[M+1]^+$ 343.75, found 343.80.

4.2.9. General procedure for the synthesis of compound ***11a-o.***

4-((5-carbamoyl-4-chloropyrimidin-2-yl)amino)phenyl methanesulfonate **(10;** 1.0 eq) was dissolved in dioxane (40 mL) and DIPEA (1.1 eq) was added to the reaction mixture at 0°C followed by the addition of different amines (1.0 eq). The reaction mixture was stirred at 0°C for 6 hr. After completion of reaction, the mixture was diluted with water and the compound was extracted in EtOAc. Organic layer was dried over sodium sulfate, filtered and concentrated under vacuum to afford the crude product. Crude product was purified by flash chromatography over silica gel (100-200 mesh), with 2 % MeOH/$CHCl_3$ to provide the desired title product **(11a-o)**.

4.2.9.1. 4-((4-Amino-5-carbamoylpyrimidin-2-yl)amino)phenyl methanesulfonate ***(11a).*** Refer to the general procedure for the synthesis of **11a**, as described in section 4.1.9. 49.4% isolated yield; white solid. ^{1}H NMR (DMSO-d_6, 400 MHz) δ ppm 3.33 (s, 3H), 7.22 (d, *J = 9.2 Hz*, 2H), 7.89 (d, *J = 9.2 Hz*, 2H), 8.54 (s, 1H), 9.58 (s, 1H). ^{13}C NMR (DMSO-d6, 100 MHz) δ ppm 37.4, 100.1, 120.8, 122.3, 140.2, 142.9, 155.1, 158.2, 160.5, 161.8. ESI-MS: m/z Calcd for $C_{12}H_{13}N_5O_4S$ $[M]^+$ 323.33, found 323.80.

4.2.9.2. 4-((5-Carbamoyl-4-(cyclopropylamino)pyrimidin-2-yl)amino)phenyl methanesulfonate ***(11b).*** Refer to the general procedure for the synthesis of **11b**, as described in section 4.1.9. 48.9% isolated yield; white solid. ^{1}H NMR (DMSO-d_6, 400 MHz) δ ppm 0.54 (t, *J = 3.0 Hz*, 2H), 0.84 (t, *J = 3.4 Hz*, 2H), 2.66 - 2.67 (m, 1H), 3.32 (s, 3H), 7.26 (d, *J = 9.2 Hz*, 2H), 8.02 (d, *J = 8.8 Hz*, 2H), 8.53 (s, 1H), 9.22 (s, 1H), 9.75 (s, 1H). ^{13}C NMR (DMSO-d6, 100 MHz) δ ppm 7.5, 25.0, 37.1, 100.5, 121.0, 122.5, 140.5, 144.0, 158.2, 160.4, 161.8, 169.4. ESI-MS: m/z Calcd for $C_{15}H_{18}N_5O_4S$ $[M+1]^+$ 364.39, found 364.00.

4.2.9.3. 4-((5-Carbamoyl-4-(cyclobutylamino)pyrimidin-2-yl)amino)phenyl methane sulfonate ***(11c).*** Refer to the general procedure for the synthesis of **11c**, as described in section 4.1.9. 49.7% isolated yield; white solid. ^{1}H NMR (DMSO-d_6, 400 MHz) δ ppm 1.25 (m, 2H), 1.78 (m, 2H), 2.37 (m, 2H), 3.33 (s, 3H), 4.51- 4.55 (m, 1H), 7.28 (d, *J* = *9.2 Hz*, 2H), 7.87 (d, *J* = *9.2 Hz*, 2H), 8.53 (s, 1H), 9.30 (d, *J* = *7.2 Hz*, 1H), 9.67 (s, 1H). ^{13}C NMR (DMSO-d6, 100 MHz) δ ppm 12.5, 30.2, 37.3, 51.2, 100.8, 121.5, 122.3, 140.1, 144.5, 158.8, 160.9, 161.7, 169.3. ESI-MS: m/z Calcd for $C_{16}H_{20}N_5O_4S$ $[M+1]^+$ 378.42, found 378.00.

4.2.9.4. 4-((5-Carbamoyl-4-(cyclopentylamino)pyrimidin-2yl)amino) phenylmethane sulfonate ***(11d).*** Refer to the general procedure for the synthesis of **11d**, as described in section 4.1.9. 48.2% isolated yield; white solid. ^{1}H NMR (DMSO-d_6, 400 MHz) δ ppm 1.46 - 149 (m, 2H), 1.50 - 173 (m, 4H), 1.98 - 2.06 (m, 2H), 3.32 (s, 3H), 4.30 - 4.38 (m, 1H), 7.25 (d, *J = 9.2 Hz*, 2H), 7.88 (d, *J = 9.2 Hz*, 2H), 8.52 (s, 1H), 9.20 (d, *J = 7.2 Hz*, 1H), 9.65 (s, 1H). ^{13}C NMR (DMSO-d6, 100 MHz) δ ppm 23.8, 33.2, 37.5, 52.0, 100.2, 120.4, 122.6, 140.1, 143.5, 157.5, 160.2, 161.4, 169.5. ESI-MS: m/z Calcd for $C_{17}H_{22}N_5O_4S$ $[M+1]^+$ 392.45, found 392.00.

*4.2.9.5. 4-((5-Carbamoyl-4-(cyclohexylamino)pyrimidin-2-yl)amino) phenylmethanes sulfonate **(11e).*** Refer to the general procedure for the synthesis of **11e**, as described in section 4.1.9. 47.5% isolated yield; white solid. ^{1}H NMR (DMSO-d_6, 400 MHz) δ ppm 1.24 - 1.31 (m, 3H), 1.35 - 1.44 (m, 2H), 1.62 - 1.59 (m, 1H), 1.70 - 1.73 (m, 2H), 1.95 - 1.98 (m, 2H), 3.33 (s, 3H), 3.93 - 3.94 (m, 1H), 7.25 (d, *J = 9.2 Hz*, 2H), 7.86 (d, *J = 8.8 Hz*, 2H), 8.52 (s, 1H), 9.17 (d, *J = 7.2 Hz*, 1H), 9.66 (s, 1H). ^{13}C NMR (DMSO-d6, 100 MHz) δ ppm 24.8, 25.7, 32.6, 37.5, 49.0, 100.0, 120.3, 122.6, 140.1, 143.5, 157.7, 160.3, 161.0, 169.6. ESI-MS: m/z Calcd for $C_{18}H_{24}N_5O_4S$ $[M+1]^+$ 406.47, found 406.00.

*4.2.9.6. 4-((5-Carbamoyl-4-((cyclopentylmethyl)amino)pyrimidin-2-yl)amino)phenylmethane sulfonate **(11f).*** Refer to the general procedure for the synthesis of **11f**, as described in section 4.1.9. 48.2% isolated yield; white solid. ^{1}H NMR (DMSO-d_6, 400 MHz) δ ppm 1.18 - 1.22 (m, 2H), 1.53 - 155 (m, 2H), 1.56 - 160 (m, 2H), 1.62 - 1.75 (m, 2H), 1.98 - 2.00 (m, 1H), 3.51 (s, 5H), 7.28 (d, *J = 8.8 Hz*, 2H), 7.85 (d, *J = 8.0 Hz*, 2H), 8.51 (s, 1H), 9.40 (s, 1H), 9.85 (s, 1H). ^{13}C NMR (DMSO-d6, 100 MHz) δ ppm 25.2, 30.3, 37.5, 45.3, 100.5, 120.9, 122.8, 139.4, 143.9, 158.9, 159.4, 161.8, 169.1. ESI-MS: m/z Calcd for $C_{18}H_{24}N_5O_4S$ $[M+1]^+$ 406.47, found 406.30.

*4.2.9.7. 4-((5-Carbamoyl-4-(isobutylamino)pyrimidin-2-yl)amino)phenyl methanesulfonate **(11g).*** Refer to the general procedure for the synthesis of **11g**, as described in section 4.1.9. 46.3% isolated yield; white solid. ^{1}H NMR (DMSO-d_6, 400 MHz) δ ppm 0. 93 (d, *J = 6.8 Hz*, 6H), 3.10 (s, 2H), 3.33 (s, 3H), 4.10 - 4.15 (m, 1H), 7.25 (d, *J = 9.2 Hz*, 2H), 7.87 (d, *J = 9.2 Hz*, 2H), 8.53 (s, 1H), 9.38 (s, 1H), 9.66 (s, 1H). ^{13}C NMR (DMSO-d6, 100 MHz) δ ppm 21.3, 29.9, 37.4, 49.2, 100.1, 121.2, 122.0, 139.6, 144.0, 159.0, 159.9, 161.9, 169.4. ESI-MS: m/z Calcd for $C_{16}H_{21}N_5O_4S$ $[M]^+$ 379.44, found 379.50.

*4.2.9.8. 4-((5-Carbamoyl-4-((3-methylbutan-2-yl)amino)pyrimidin-2-yl)amino)phenyl methane sulfonate **(11h).*** Refer to the general procedure for the synthesis of **11h**, as described in section 4.1.9. 48.1% isolated yield; white solid. ^{1}H NMR (DMSO-d_6, 400 MHz) δ ppm 0.90 (d, *J = 6.8 Hz*, 3H), 0.94 (d, *J = 6.8 Hz*, 3H), 1.13 (d, *J = 6.8 Hz*, 3H), 1.85 - 1.90 (m, 1H), 3.34 (s, 3H), 4.06 - 4.11 (m, 1H), 7.26 (d, *J = 9.2 Hz*, 2H), 7.85 (d, *J = 9.2 Hz*, 2H), 8.53 (s, 1H), 9.27 (d, *J = 8.4 Hz*, 3H), 9.65(s,1H). ^{13}C NMR (DMSO-d6, 100 MHz) δ ppm 16.6, 18.0, 18.4, 31.9, 37.1, 50.1, 99.5, 119.9, 122.2, 139.6, 143.1, 157.1, 159.8, 161.0, 169.2. ESI-MS: m/z Calcd for $C_{17}H_{24}N_5O_4S$ $[M+1]^+$ 394.46, found 394.20.

4.2.9.9. (R)-4-((5-Carbamoyl-4-((3-methylbutan-2-yl)amino)pyrimidin-2-yl)amino) phenyl methane sulfonate ***(11i).*** Refer to the general procedure for the synthesis of **11i**, as described in section 4.1.9. 47.4% isolated yield; white solid. ^{1}H NMR (DMSO-d_6, 400 MHz) δ ppm 0.90 (d, *J = 6.8 Hz*, 3H), 0.94 (d, *J = 6.8 Hz*, 3H), 1.13 (d, *J = 6.4 Hz*, 3H,), 1.84 - 1.92 (m ,1H), 3.34 (s, 3H), 4.05 - 4.12 (m ,1H), 7.26 (d, *J = 9.2 Hz*, 2H), 7.87 (d, *J = 9.2 Hz*, 1H), 8.54 (s, 1H), 9.28 (d, *J = 8.4 Hz,* 2H), 9.64 (s, 1H). ^{13}C NMR (DMSO-d6, 100 MHz) δ ppm 17.1, 18.4, 18.8, 32.4, 37.5, 50.6, 100.0, 120.3, 122.6, 140.0, 143.5, 157.7, 160.3, 161.5, 169.7. ESI-MS: m/z Calcd for $C_{17}H_{24}N_5O_4S$ $[M+1]^+$ 394.46, found 394.14.

4.2.9.10. (S)-4-((5-Carbamoyl-4-((3-methylbutan-2-yl)amino)pyrimidin-2-yl)amino) phenyl methane sulfonate ***(11j).*** Refer to the general procedure for the synthesis of **11j**, as described in section 4.1.9. 47.4% isolated yield; white solid. ^{1}H NMR (DMSO-d_6, 400 MHz) δ ppm 0.88 (d, *J = 6.8 Hz*, 3H), 0.94 (d, J = *6.8 Hz*, 3H), 1.12 (d, J = *6.8 Hz*, 3H), 1.85 - 1.89 (m, 1H), 3.33(s, 1H), 4.06 - 4.11 (m, 1H), 7.26 (d, *J = 9.2 Hz*, 2H) 7.85 (d, *J = 9.2 Hz*, 2H), 8.52 (s, 1H), 9.27 (d, *J = 8.4 Hz*, 1H), 9.64 (s, 1H). ^{13}C NMR (DMSO-d6, 100 MHz) δ ppm 16.9, 18.1, 18.6, 32.1, 37.3, 50.2, 100.1, 120.1, 122.3, 140.1, 143.4, 157.5, 160.0, 161.2, 169.5. ESI-MS: m/z Calcd for $C_{17}H_{24}N_5O_4S$ $[M+1]^+$ 394.46, found 394.20.

4.29.11. (R)-4-((5-Carbamoyl-4-((1-phenylethyl)amino)pyrimidin-2-yl)amino)phenyl methane sulfonate ***(11k)***. Refer to the general procedure for the synthesis of **11k**, as described in section 4.1.9. 47.8% isolated yield; white solid. ^{1}H NMR (DMSO-d_6, 400 MHz) δ ppm 1.48 (d*, J = 8.2 Hz*, 3H), 3.32 (s, 3H), 5.20 - 5.23 (m, 1H), 7.21-7.16 (m, 3H), 7.23 - 7.42 (m, 4H), 7.60 - 7.66 (m, 2H), 8.55 (s, 1H), 9.63 (m, 2H). ^{13}C NMR (DMSO-d6, 100 MHz) δ ppm 20.9, 37.4, 55.2, 100.4, 121.1, 122.7, 127.1, 127.9, 128.7, 139.7, 140.3, 143.9, 158.5, 160.8, 162.2, 169.8. ESI-MS: m/z Calcd for $C_{20}H_{21}N_5O_4S$ $[M]^+$ 427.48, found 427.80.

4.2.9.12. 4-((5-Carbamoyl-4-((3-fluorobenzyl)amino)pyrimidin-2-yl)amino)phenyl methane sulfonate ***(11l)***. Refer to the general procedure for the synthesis of **11l**, as described in section 4.1.9. 46.2% isolated yield; white solid. ^{1}H NMR (DMSO-d_6, 400 MHz) δ ppm 3.33 (s, 3H), 4.67 (d, *J = 6.0 Hz*, 2H), 7.04 - 7.19 (m. 5H), 7.35 - 7.41 (m, 1H), 7.68 (d, *J = 9.2 Hz*, 2H), 8.57 (s, 1H), 9.59 (t, *J = 5.6 Hz*, 2H), 9.68 (s, 1H). ^{13}C NMR (DMSO-d6, 100 MHz) δ ppm 37.6, 43.7, 100.3, 112.5, 117.9, 121.1, 122.8, 123.1, 127.0, 139.5, 142.1, 143.8, 158.2, 159.9, 160.9, 162.0, 169.6. ESI-MS: m/z Calcd for $C_{19}H_{18}FN_5O_4S$ [M]+ 431.44, found 431.80.

*4.2.9.13. 4-((5-Carbamoyl-4-((4-fluorobenzyl)amino)pyrimidin-2-yl)amino)phenyl methane sulfonate **(11m)***. Refer to the general procedure for the synthesis of **11m**, as described in section 4.1.9. 47.3% isolated yield; white solid. ^{1}H NMR (DMSO-d$_6$, 400 MHz) δ ppm 3.32 (s, 3H), 4.67 (d, *J = 6.0 Hz*, 2H), 7.15 - 7.20 (m, 4H), 7.35 - 7.39 (m, 2H), 7.72 (d, *J = 8.8 Hz*, 2H), 8.56 (s, 1H), 9.55 (s, 1H), 9.67 (s, 1H). ^{13}C NMR (DMSO-d6, 100 MHz) δ ppm 37.5, 43.4, 100.5, 115.2, 121.0, 122.5, 127.7, 139.2, 140.3, 143.2, 159.4, 160.2, 160.8, 162.3, 169.1. ESI-MS: m/z Calcd for $C_{19}H_{18}FN_5O_4S$ [M]+ 431.44, found 431.90.

*4.2.9.14. 4-((5-Carbamoyl-4-((2-fluorobenzyl)amino)pyrimidin-2-yl)amino)phenyl methane sulfonate **(11n)*** Refer to the general procedure for the synthesis of **11n**, as described in section 4.1.9. 47.9% isolated yield; white solid. ^{1}H NMR (DMSO-d$_6$, 400 MHz) δ ppm 3.32 (s, 3H), 4.67 (d, *J = 6 Hz*, 2H), 7.13 - 7.17 (m, 3H), 7.21 - 7.33 (m, 3H), 7.69 (d, *J = 8.8 Hz*, 2H), 8.57 (s, 1H), 9.55 (s, 1H), 9.67 (s, 1H). ^{13}C NMR (DMSO-d6, 100 MHz) δ ppm 37.2, 39.3, 100.6, 114.7, 121.4, 122.8, 124.0, 128.1, 129.5, 139.0, 139.2, 143.5, 159.2, 160.5, 161.2, 162.9, 169.7. ESI-MS: m/z Calcd for $C_{19}H_{18}FN_5O_4S$ $[M]^+$ 431.44, found 431.90.

*4.2.9.15. 4-((5-Carbamoyl-4-((naphthalen-1-ylmethyl)amino)pyrimidin-2-yl)amino) phenyl methanes ulfonate **(11o)***. Refer to the general procedure for the synthesis of **11o**, as described in section 4.1.9. 50.5% isolated yield; white solid.^{1}H NMR (DMSO-d$_6$, 400 MHz) δ ppm 1.67 (d, *J = 6.8 Hz*, 3H), 3.28 (s, 3H), 6.05 (t, *J = 6.4 Hz*, 1H), 6.52 - 6.58 (m, 2H), 7.36 - 7.44 (m, 2H), 7.45 - 7.48 (m, 2H), 7.64 - 7.85 (m, 2H), 7.89 -7.91 (m, 1H), 8.01 (d, *J = 8.0 Hz*, 1H), 8.27 (d, *J = 8.4 Hz*, 1H), 8.59 (s, 1H), 8.97 (s, 1H), 9.83 (s, 1H), 12.90 (d, *J* = 9.2 Hz, 1H). ^{13}C NMR (DMSO-d6, 100 MHz) δ ppm 21.5, 37.6, 57.9, 100.2, 121.8, 122.4, 122.9, 125.8, 126.9, 128.1, 131.0, 139.4, 140.9, 143.5, 159.7, 161.0, 162.7, 169.2. ESI-MS: Calcd for $C_{24}H_{25}N_5O_4S$ $[M+2]^+$ 477.54, found 479.21.

4.3. In vitro and ex vivo assay:

4.3.1: Enzymatic potency of JAK inhibitors (biochemical assay):

Human JAK1-3 and TYK2 kinase domains were purchased from Carna Biosciences (Japan), and the assay was performed using a streptavidin-coated 96-well plate. The reaction mixture contained 15 mM Tris-HCl (pH 7.5), 0.01% Tween 20, 2 mM DTT, 10 mM $MgCl_2$, 250 nM Biotin-Lyn-Substrate-2 (Peptide Institute, Inc., Osaka, Japan) and ATP. The final concentrations of ATP were 10 μM for JAK1-3 and TYK2. Test compounds were dissolved in DMSO and the reaction was initiated by adding the kinase domain, followed by incubation at room temperature for 1 hr. Kinase activity was measured as the rate of phosphorylation of Biotin-Lyn-Substrate-2, using HRP-conjugated anti-phosphotyrosine antibody (HRP-PY-20; Santa Cruz Biotechnology, CA, USA) with a phosphotyrosine-specific ELISA. All the experiments were performed in duplicate. The IC_{50} values were calculated using linear regression analysis [32].

4.3.2. JAK cellular assays using human peripheral blood mononuclear cells (PBMCs):

PBMCs were collected from healthy volunteers (as per Zydus Research Centre, ethical committee protocol), into sodium heparin vacutainer tubes. After incubation with compound **11i** and Tofacitinib at 37°C for 30 min, blood was triggered with either recombinant human IL-6 (400 ng/mL; R&D Systems), IL-2 (20 ng/mL; R&D Systems), GM-CSF (100 ng/mL; Pepro-Tech), or vehicle (PBS plus 0.1% [w/v] BSA), at 37°C for 20 min and treated with pre-warmed 13 lysis/fix buffer (BD Biosciences) to lyse RBCs and fix leukocytes. Cells were permeabilized with 100% MeOH and incubated with anti-pSTAT3 and anti-CD4 (IL- 6-triggered samples), anti-pSTAT5 and anti-CD4 Abs (IL-2-triggered samples), or anti-pSTAT5 Abs (GM-CSF-triggered samples; all Abs were from BD Biosciences) at 4°C, for 30min, washed once with PBS and analyzed on a FACS Canto II flow cytometer.[33, 34] IC_{50} values were determined, using Prism software (Version 7, GraphPad), for Tofacitinib and **11i**, Table 4.

4.3.3. Plasma protein binding:

An equilibrium dialysis method was used to determine the plasma fraction unbound (fu) values. Briefly, dialysis membranes (MWCO 12-14K) and 96-well dialysis devices were assembled following the manufacturer's instructions (HT Dialysis, LLC, USA). Human plasma samples containing 1 μmol/L test compounds with 1% DMSO were dialyzed against PBS for 6 hours in a humidified incubator (75% relative humidity; 5% CO_2/95% air) at 37°C at 450 RPM. Quadruplicates of binding were measured for each compound. Samples were matrix-matched and quenched with cold acetonitrile containing internal standard(s). The solutions were centrifuged and the supernatant was analyzed using LC-MS/MS.

4.4. In vivo efficacy studies:

The animal experiments were carried out in rats and mice, bred in-house. Animals were housed in groups of 6 animals per cage, for a week, in order to habituate them to vivarium conditions (25 ± 4 ^{o}C, 60-65 % relative humidity, 12 : 12 h light dark cycle, with lights on, at 7.30 am). All the animal experiments were carried out according to the internationally valid guidelines following approval by the 'Zydus Research Center, animal ethical committee'.

4.4.1. Protocol for Collagen Induced Arthritis (CIA) study in mice:

CIA study is a representative animal model of human rheumatoid arthritis [35]. Following 7 days acclimation, male DBA1j (8 to 12-weeks old) mice were randomly assigned to groups according body weight. Mice were immunized subcutaneously in the tail using bovine type II collagen mix in complete Freund's adjuvant (CFA). Twenty-one days after the first immunization, mice were given booster dose of collagen in incomplete Freund's adjuvant (IFA). Mice were monitored every other day after the booster dose for the development of arthritis. Mice were recruited for the study once clinical signs were visible. Eight animals were assigned each of three groups [vehicle, Tofacitinib and test compound, **11i**], treatment was continued for three weeks and percentage inhibition in clinical score is recorded as per graded score. Body weights of the animals were also recorded 3 times a week as a measure of treatment related side effect and paw thickness measured twice a week (Fig. 2a). The mice were scored in a blinded manner, for signs of arthritis in each paw according to the following scale: 0 - no swelling or redness/normal paw; 1- swelling and/or redness in one digit; 2- swelling and/or redness in two or more digits; and 3- entire paw is swollen or red. The severity score was reported as the sum of all four paws for each mouse and expressed as the average severity score for each group.

4.4.2. Protocol for Adjuvant Induced Arthritis (AIA) model in rats:

Arthritis was induced in female Lewis rats by inoculation with Freund's complete adjuvant (CFA). [36] Briefly, on day 0, rats were anesthetized (mixture of ketamine and xylazine (80: 10 mg/kg, intraperitoneally)) and then injected with 0.1 mL CFA (1 mg/mL of heat-inactivated Mycobacterium tuberculosis) intra-dermally, at the base of the tail. Eight animals were assigned in each of the three groups [vehicle (2% sodium carboxymethylcellulose (CMC), positive control (Tofacitinib, 60 mg/kg) and test compound **11i** (3, 10 and 30 mg/kg)]. Treatment was continued for 20 days (once daily, by oral gavage) and paw edema determined by measuring changes in the paw volume, using a plethysmometer, on days 10, 12, 14, 16, 18 and 20, post-CFA injection. Statistical analysis was performed by one-way ANOVA (Dunnett's method, data represent the mean ± S.E.M., n = 8/group).

4.5. Pharmacokinetic studies:

A comparative single dose (3 mg/kg, po and 1 mg/kg, iv) PK study of compounds **5k**, **11i** and Tofacitinib was evaluated in overnight fasted male C57BL/6J mice (n=6). Serial blood samples were collected in the micro-centrifuge tubes containing EDTA, at pre-dose, 0.15, 0.3, 0.5, 0.75, 1, 2, 4, 6, 8, 24 and 30 h post-dose, after the compounds administration. Approximately 0.3 ml of blood was collected at each time points and centrifuged at 4^{o}C. The obtained plasma was frozen, stored at-70^{o}C and the concentrations of compounds in plasma were determined by the LC-MS/MS (Shimadzu LC10AD, USA), using YMC hydrosphere C18 (2.0 x 50 mm, 3 μm) column (YMC Inc., USA). The pharmacokinetic parameters, such as Tmax, $t_{1/2}$, Cmax, AUC and %F were calculated using a non-compartmental model of WinNonlin software version 5.2.1.

4.6. Docking studies:

Multiple structures of JAK3, co-crystallized with various ligands, were analyzed, and the structure with PDB ID 5W86 (solved at 2.6Å) was selected due to core similarity of the co-crystallized ligand and Cerdulatinib. [37] The protein was prepared using protein preparation wizard of Schrodinger Suite 2018-4, at pH 7.4. Ligands were prepared using Ligprep module at pH 7.0 ± 0.5, with default settings. Glide grid was used with default options for grid generation and Glide SP docking was used for docking simulation with default settings. The docked pose of Cerdulatinib, **5k** and **11i** was analyzed with respect to docking score, docking pose and hydrogen bonding interactions with the key region residues of the JAK3 enzyme.

Acknowledgments

Authors thank the management of Zydus Research Centre, Cadila Healthcare Ltd. for support and encouragement and the analytical department for providing analytical data.

Corresponding Author: Rajesh Bahekar

E-mail: rajeshbahekar@zyduscadila.com

Notes

The authors declare no competing financial interest.

References

1. Boyle, D.; Kim, H.; Topolewski, K.; Bartok, B.; Firestein, G. Novel Phosphoinositide 3-Kinase δ, γ Inhibitor: Potent Anti-Inflammatory Effects and Joint Protection in Models of Rheumatoid Arthritis. *J Pharmacol Exp Thera.* **2014**, 348, 271-280. DOI: 10.1124/jpet.113.205955.

2. Conigliaro, P.; Triggianese, P.; Martino, E.; Chimenti, M.; Sunzini, F.; Viola, A.; Claudia. Challenges in the treatment of Rheumatoid Arthritis. *Autoimmunity Reviews*. **2019**, 18, 706-713. DOI: 10.1016/j.autrev.2019.05.007.

3. Roskoski, R. *Pharmacological Research*. **2016**, 111, 784-803. DOI: 10.1016/j.phrs.2016.07.038.

4. Schindler, C.; Plumlee, C. Interferons pen the JAK-STAT pathway. *Seminar in Cell & Developmental Biology*. **2008**, 19, 311-318. DOI: 10.1016/j.semcdb.2008.08.010.

5. Mohr, A.; Chatain, N.; Domoszlai, T.; Rinis, N.; Sommerauer, M.; Vogt, M.; Muller-Newen, G. Dynamics and non-canonical aspects of JAK/STAT signaling. *European Journal of Cell Biology*. **2012**, 91, 524-532. DOI: 10.1016/j.ejcb.2011.09.005.

6. John, J.; Schwartz, D.; Villarino, A.; Gadina, M.; McInnes, I.; Laurence, A. The JAK-STAT pathway: impact on human disease and therapeutic. *Annu Rev Med*. **2015**, 66, 311-328. DOI: 10.1146/annurev-med-051113-024537.

7. Sailliet, N.; Brosseau, C.; Robert, J.; Brouard, S. Role of JAK inhibitors and immune cells in transplantation. *Cytokine & Growth Factor Reviews*. **2019**, 47, 62-63. DOI: 10.1016/j.cytogfr.2019.05.002.

8. Hammaren, H.; Virtanen, A.; Raivola, J.; Silvennoinen, O. The regulation of JAKs in cytokine signaling and its breakdown in disease. *Cytokine*. **2019**, 118, 48-63. DOI: 10.1016/j.cyto.2018.03.041.

9. Yan, Z.; Gibson, S.; Buckley, J.; Qin, H.; Benveniste, E. Role of JAK/STAT signaling pathway in regulation of innate immunity in neuroinflammatory diseases. *Clinical Immunology*. **2018**, 189, 4-13. DOI: 10.1016/j.clim.2016.09.014.

10. Haan, C.; Kreis, S.; Mague, C.; Behrmann, I. Jaks and Cytokine receptors – An intimate relationship. *Biochemical Pharmacology*. **2006**, 72, 1538-1546. DOI: 10.1016/j.bcp.2006.04.013.

11. Yamaoka, K.; Saharinen, P.; Pesu, M.; Holt, V.; Silvennoinen, O.; John, J. The Janus Kinases (JAKs), *Genome Biology*. **2004**, 5, 253. DOI: 10.1186/GB-2004-5-12-253.

12. Flanagan, M.; Blumenkopf, T.; Brissette, W.; Brown, M.; Casavant, j.; Shang-Poa, C.; Doty, J.; Elliott, E.; Fisher, M.; Hines, M.; Kent, C.; Kudlacz, E.; Lillie, B.; Magnuson, K.; McCurdy, S.; Munchhof, M.; Perry, B.; Sawyer, P.; Strelevitz, T.; Subramanyam, C.; Sun, J.; Whipple, D.; Changelian, P. Discovery of CP-690,550: Apotent and selective Janus Kinase (JAK) inhibitor for the treatment of Autoimmune Diseases and Organ Transplant Rejection. *J. Med. Chem*. **2010**, 53, 8468-8484. DOI: 10.1021/jm1004286.

13. Elliott, N.; Cleveland, S.; Grann, V.; Janik, J.; Waldmann, T.; Dave, U. FERM domain mutations induce gain of function in JAK3 in adult T-Cell leukemia/lymphoma. *Bood*. **2011**, 118, 3911-3921. DOI: 10.1182/blood-2010-12-319467.

14. Chen, M.; Cheng, A.; Chen, Y.; Hymel, A.; Hanson, E.; Kimmel, L.; Minami, Y.; Taniguchi, T.; Changelian, P.; John, J. The amino terminus of JAK3 is necessary and sufficient for binding to the common γ Chain and confers the ability to transmit interleukin 2- mediated signals. *Immunology*. **1997**, 94, 6910-6915. DOI: 10.1073/pnas.94.13.6910.

15. Genovese, M.; Slomen, J.; Weinblatt, M.; Burmester, G.; Meerwein, S.; Camp, H.; Wang, L.; Othman, A.; Khan, N.; Pangan, A.; Jungerwirth, S. Efficacy and safety of ABT-494, a Selective JAK-1 inhibitor, in a Phase llb study in Patients with Rheumatoid Arthritis and an lnadequate Response to Methotrexate. *Arthritis & Rheumatology*. **2016**, 68, 2857-2866. DOI: 10.1002/art.39808.

16. Gadina, M.; Lel, M.; Schwartz, D.; Silvennoinen, O.; Nkayamada S.; Yamaoka, K.; John, J.

Janus kinase to jakinibs: from basic insights to clinical practice. *Rheumatology*. **2019**, 58, i14-i16. DOI: 10.1093/rheumatology/key432.

17. Thoma, G.; Druckes, P.; Zerwes, H. Selective inhibitors of the Janus Kinase JAK3 - Are they effective? *Bioorg. Med. Chem. Lett*. **2014**, 24, 4617-4621. DOI: 10.1016/j.bmcl.2014.08.046.

18. Clark, M.; George, K.; Bookland, R.; Chen, J.; Laughlin, S.; Thakur, K.; Lee, W.; Davis, J.; Cabrera, E.; Brugel, T.; VanRens, J.; Laufersweiler, M.; Maier, J.; Sabat, M.; Golebiowski, A.; Easwaran, V.; Webster, M.; Dea, B.; Zhanga, G. Development of new pyrrolopyrimidine-based inhibitors of Janus kinase 3 (JAK3). *Bioorg. Med. Chem. Lett*. **2007**, 17, 1250-1253. DOI: 10.1016/j.bmcl.2006.12.018.

19. Nakajima, Y.; Inoue, T.; Nakai, K.; Mukoyoshi, K.; Hamaguchi, H.; Hatanaka, K.; Sasaki, H.; Tanaka, A.; Takahashi, F.; Kunikawa, S.; Usuda, H.; Moritomo, A.; Higashi, Y.; Inami, M.; Shirakami. S. Synthesis and evaluation of novel 1H-pyrrolo [2,3-b] pyrimidine -5- carboxamide derivatives as potent and orally efficacious immunomodulatois targeting JAK 3. *Bioorg. Med. Chem*. **2015**, 23, 4871-4883. DOI: 10.1016/j.bmc.2015.05.034.

20. Yamagishi, H.; Shirakami, S.; Nakajima, Y.; Tanaka, A.; Takahashi, F.; Hamaguchi, H.; Hatanaka, K.; Moritomo, A.; Inami, M.; Higashi, Y.; Inoue, T. Discovery of

3,6dihydroimidazo[4,5-d] pyrrolo [2,3-b] pyridine - 2 (1H) – one derivatives as novel JAK inhibitors. *Bioorg. Med. Chem*. **2015**, 23, 4846-4859. DOI: 10.1016/j.bmc.2015.05.028.

21. Kaur, K.; Kalra, S.; Kaushak, S. Systematic Review of Tofacitinib: A new Drug for the Management of Rheumatoid Arthritis. *Clinical Therapeutics*. **2014**, 36, 1074-1086. DOI: 10.1016/j.clinthera.2014.06.018.

22. Sanchez, G.; Reinhardt, A.; Ramsey, S.; Wittkowski, H.; Hashkes, P.; Berkun, Y.; Schalm, S.; Murias, S.; Dare, J.; Brown, D.; Stone, D.; Gao, L.; Klausmeier, T.; Foell, D.; Jesus, A.; Chapelle, D.; Kim, H.; Dill, S.; Colbert, R.; Failla, L.; Kost, B.; O'Brien, M.; Reynolds, J.; Folio, L.; Calvo, K.; Paul, S.; Weir, N.; Brofferio, A.; Soldatos, A.; Biancotto, A.; Cowen, E.; Digiovanna, J.; Gadina, M.; Lipton, A.; Hadigan, C.; Holland, S.; Fontana, J.; Alawad, A.; Brown, R.; Rother, K.; Heller, T.; Brooks, K.; Kumar, P.; Brooks, S.; Waldman, M.; Singh, H.; Nickeleit, V.; Silk, M.; Prakash, A.; Janes, J.; Ozen, S.; Wakim, P.; Brogan, P.; Macias, W.; Goldbach-Mansky, R. Jak1/2 inhibition with baricitinib in the treatment of autoinflammatory interferonopathies. *The Journal of Clinical Investigation*. **2018**, 28, 3041-3052. DOI: 10.1172/JCI98814.

23. Harrison, C.; Vannucchi, A.; Platzbecker, U.; Cervantes, F.; Gupta, V.; Lavie, D.; Passamonti, F.; Winton, E.; Dong, H.; Kawashima, J.; Maltzman, J.; Kiladjian, j.; Verstovsek, S. Momelotinib versus best available therapy in patients with myelofibrosis previously treated with ruxolitinib (SIMPLIFY 2): a randomised, open-label, phase 3 trial. *The Lancet haematology*. **2018**, 5, e73-e8. DOI: 10.1016/S2352-3026(17)30237-5.

24. Harrison, C.; Schaap, N.; Vannucchi, A.; Kiladjian, J.; Tiu, R.; Zachee, P.; Jourdan, E.; Winton, E.; Silver, R.; Schouten, H.; Passamonti, F.; Zweegman, S.; Talpaz, M.; Lager, J.; Shun, Z.; Mesa, R. Janus kinase-2 inhibitor fedratinib in patients with myelofibrosis previously treated with ruxolitinib (JAKARTA-2): a single-arm, open-label, non-randomised, phase 2, multicentre study. *The Lancet haematology*. **2017**, 4, e317-e324. DOI: 10.1016/S2352-3026(17)30088-1.

25. Blunt, M.; Koehrer, S.; Dobson, R.; Larrayoz, M.; Wilmore, S.; Hayman, A.; Parnell, J.; Smith, L.; Davies, A.; Johnson, P.; Conley, P.; Pandey, A.; Strefford, J.; Stevenson, F.; Packham, G.; Forconil, F.; Coffey, G.; Burger, J.; Steele, A. The dual syk/JAK inhibitor cerdulatinib antagonises B-cell receptor and microenvironment signaling in chronic lymphocytic leukemia. *Clin Cancer Res*. **2017**, 23, 2313-2324. DOI: 10.1158/1078-0432.CCR-16-1662.

26. Lynch, S.; DeVicente, J.; Hermann, J.; Jaime-Figueroa, S.; Jin, S.; Kuglstatter, A.; Li, H.; Lovey, A.; Menke, J.; Niu, L.; Patel, V.; Roy, D.; Soth, M.; Steiner, S.; Tivitmahaisoon, P.; Vu, M.; Yee, C. Strategic use of conformational bias and structure based design to identify potent JAK 3 inhibitors with improved selectivity against the JAK family and kinome. *Bioorg. Med. Chem. Lett*. **2013**, 23, 2793-2800. DOI: 10.1016/j.bmcl.2013.02.012.

27. Goedken, E. R.; Argiriadi, M. A.; Banach, D. L.; Fiamengo, B. A.; Foley, S. E.; Frank, K. E.; George, J. S.; Harris, C. M.; Hobson, A. D.; Ihle, D. C.; Marcotte, D.; Merta, P. J.; Michalak, M.

E.; Murdock, S. E.; Tomlinson, M. J.; Voss, J. W. Tricyclic covalent inhibitors selectively target JAK3 through an active site thiol. *J. Biol. Chem*. **2015**, 290, 4573-4589. DOI: 10.1074/jbc.M114.595181.

28. Tan, L.; Akahane, K.; McNally, R.; Reyskens, K. M. S. E.; Ficarro, S. B.; Liu, S.; Herter-Sprie, G. S.; Koyama, S.; Pattison, M. J.; Labella, K.; Johannessen, L.; Akbay, E. A.; Wong, K.-K.; Frank, D. A.; Marto, J. A.; Look, T. A.; Arthur, J. S. C.; Eck, M. J.; Gray, N. S. Development of selective covalent Janus kinase 3 inhibitors. *J. Med. Chem.* **2015**, 58, 6589-6606. DOI: 10.1021/acs.jmedchem.5b00710.

29. Thorarensen, A.; Dowty, M. E.; Banker, M. E.; Juba, B.; Jussif, J.; Lin, T.; Vincent, F.; Czerwinski, R. M.; Casimiro-Garcia, A.; Unwalla, R.; Trujillo, J. I.; Liang, S.; Balbo, P.; Che, Y.; Gilbert, A. M.; Brown, M. F.; Hayward, M.; Montgomery, J.; Leung, L.; Yang, X.; Soucy, S.; Hegen, M.; Coe, J.; Langille, J.; Vajdos, F.; Chrencik, J.; Telliez, J.-B. Design of a Janus Kinase 3 (JAK3) Specific inhibitor 1-((2S,5R)-5- ((7H-pyrrolo[2,3-D]pyrimidin-4-yl)amino)-2-methylpiperidin-1-yl)- prop-2-en-1-one (PF-06651600) allowing for the interrogation of JAK3 signaling in humans. *J. Med. Chem.* **2017**, 60, 1971-1993. DOI: 10.1021/acs.jmedchem.6b01694.

30. London N, Miller RM, Krishnan S, Uchida K, Irwin JJ, Eidam O, Gibold L, Cimermancic P, Bonnet R, Shoichet BK, et al. (2014) Covalent docking of large libraries for the discovery of chemical probes. *Nat Chem Biol* **2014**, 10: 1066–1072. DOI: 10.1038/nchembio.1666.

31. Pravin, T.; Anil, A.; Mukul, J.; Sanjay, G. Heterocyclic Compounds. WO 2013/054351 A1.

32. Malerich, J.; Lam, J.; Hart, B.; Fine, R.; Klebansky, B.; Tanga, M.; D'Andrea, A. Diamino-1,2,4-triazole derivatives are selective inhibitors of TYK2 and JAK1 over JAK2 and JAK3. *Bioorg. Med. Chem. Lett*. **2010**, 20, 7454-7457. DOI: 10.1016/j.bmcl.2010.10.026.

33. Lin, T.; Hegen, M.; Quadros, E.; Nickerson-Nutter, C.; Appell, K.; Cole, A.; Shao, Y.; Tam, S.; Ohlmeyer, M.; Wang, B.; Goodwin, D.; Kimble, E.; Quintero, J.; Gao, M.; Symanowicz, P.; Wrocklage, C.; Lussier, J.; Schelling, S.; Hewet, A.; Xuan, D.; Krykbaev, R.; Togias, J.; Xu, X.; Harrison, R.; Mansour, T.; Collins, M.; Clark, J.; Webb, M.; Seidl, K. Selective functional inhibition of JAK-3 is sufficient for efficacy in collagen-induced arthritis in mice. *Arthritis Rheum.* **2010**, 62, 2283-2293. DIO: 10.1002/art.27536.

34. Botta, A.; Sirignano, E.; Popolo, A.; Saturnino, C.; Terracciano, S.; Foglia, A.; Sinicropi, M.; Longo, P.; Di Micco, S. Identification of Lead Compounds as Inhibitors of STAT3: Design, Synthesis and Bioactivity. *Mol. Inform*. **2015**, 34, 689-697.DIO: org/10.1002/minf.201500043.

35. Zhao, Y.; Liu, Y.; Zhou, D.; Dai, Q.; Liu, S. Anti-Arthritic Effect of Chebulanin on Collagen-Induced Arthritis in Mice. *Plos One* **2015**, 1-14. DOI: 10.1371/journal.pone.0139052.

36. Bevaart, L.; Vervoordeldonk, M.; Tak, P. Evaluation of therapeutic targets in animal models of arthritis: How does it relate to rheumatoid arthritis? *Arthritis & Rheumatism* **2010**, 62, 2192-2205. DOI: 10.1002/art.27503.

37. Schrödinger Release, 2018-3: Glide, Schrödinger, LLC, New York, NY, **2018**.

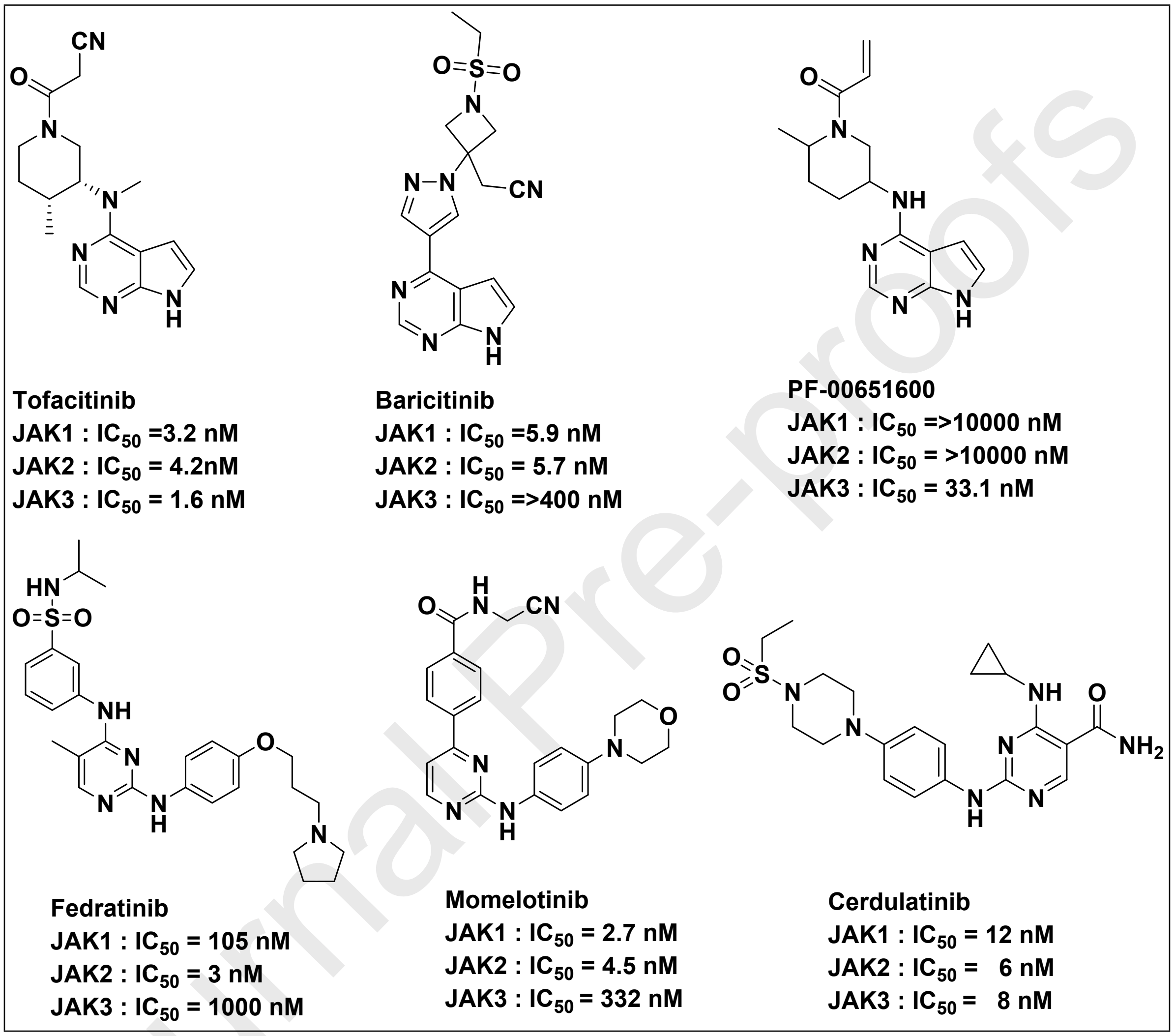

Fig. 1. Structures of 1H-pyrrolo[2,3-b]pyridine and Pyrimidine based JAK inhibitors

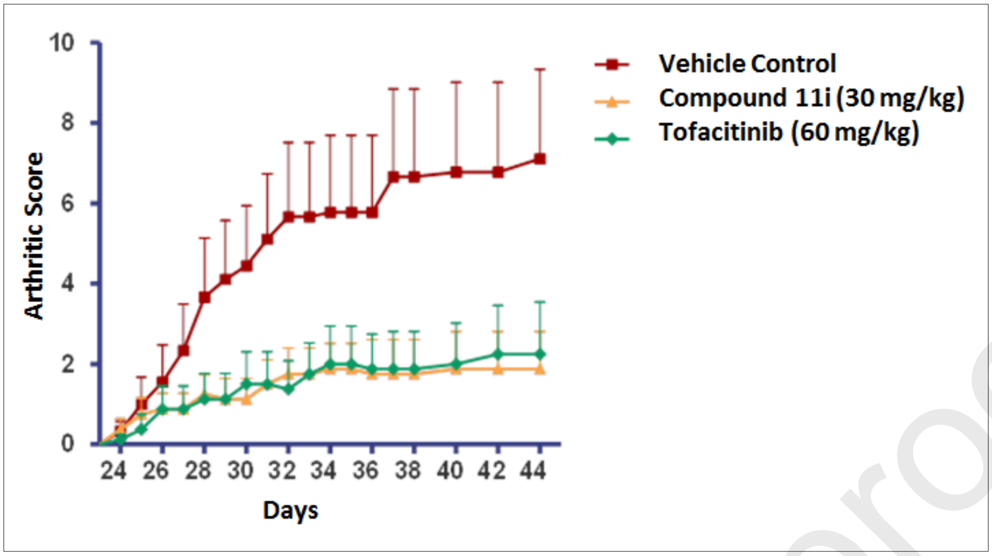

Fig. 2a. Effect of Compound **11i** and Tofacitinib in CIA mice model

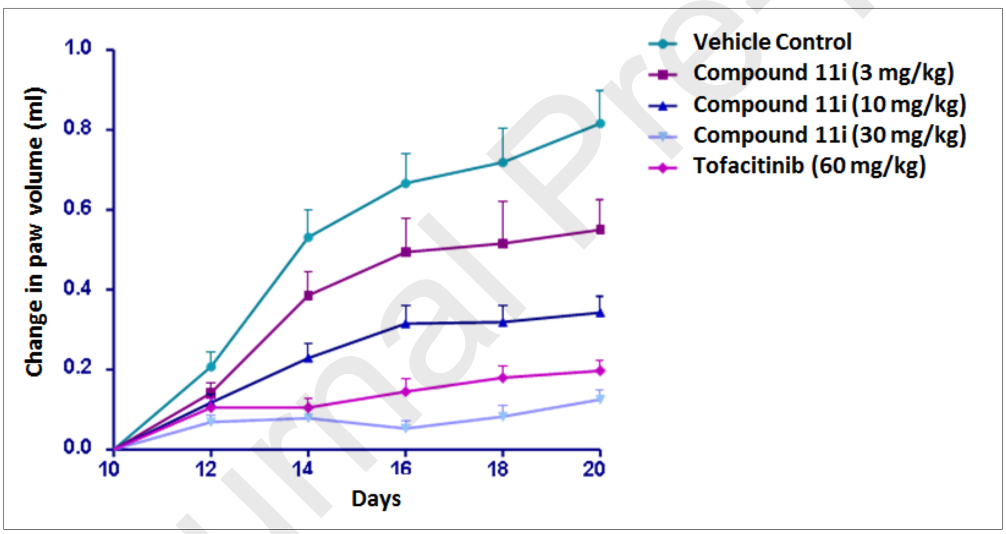

Fig. 2b. Effect of Compound **11i** and Tofacitinib in AIA rat model

A

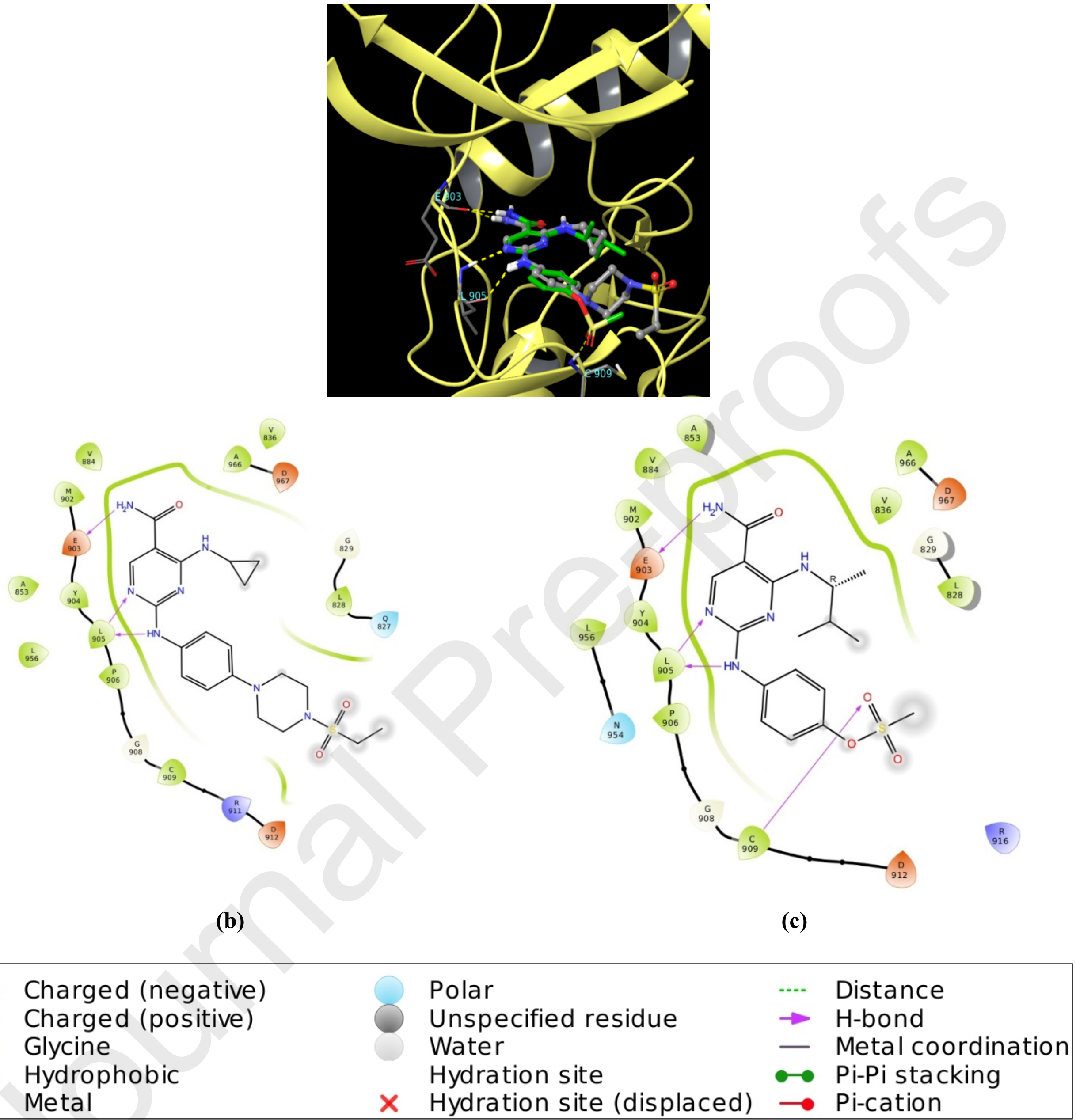

Fig. 3. Docked pose of **Cerdulatinib** and **11i** within ATP binding site of JAK3 molecular surface (PDB ID: 5W86 @2.6Å).

(a) Docked pose of Cerdulatinib and **11i** superimposed (Cerdulatinib is shown in ball and stick model with grey carbon while **11i** is displayed in stick model with green carbon), yellow dashed lines shows the H-bond interactions. (b) 2D Ligand interaction diagram of Cerdulatinib and (c) 2D Ligand interaction diagram of **11i** (carbon is shown in grey), with residues within 4Å, hydrogen bonds are shown with arrows.

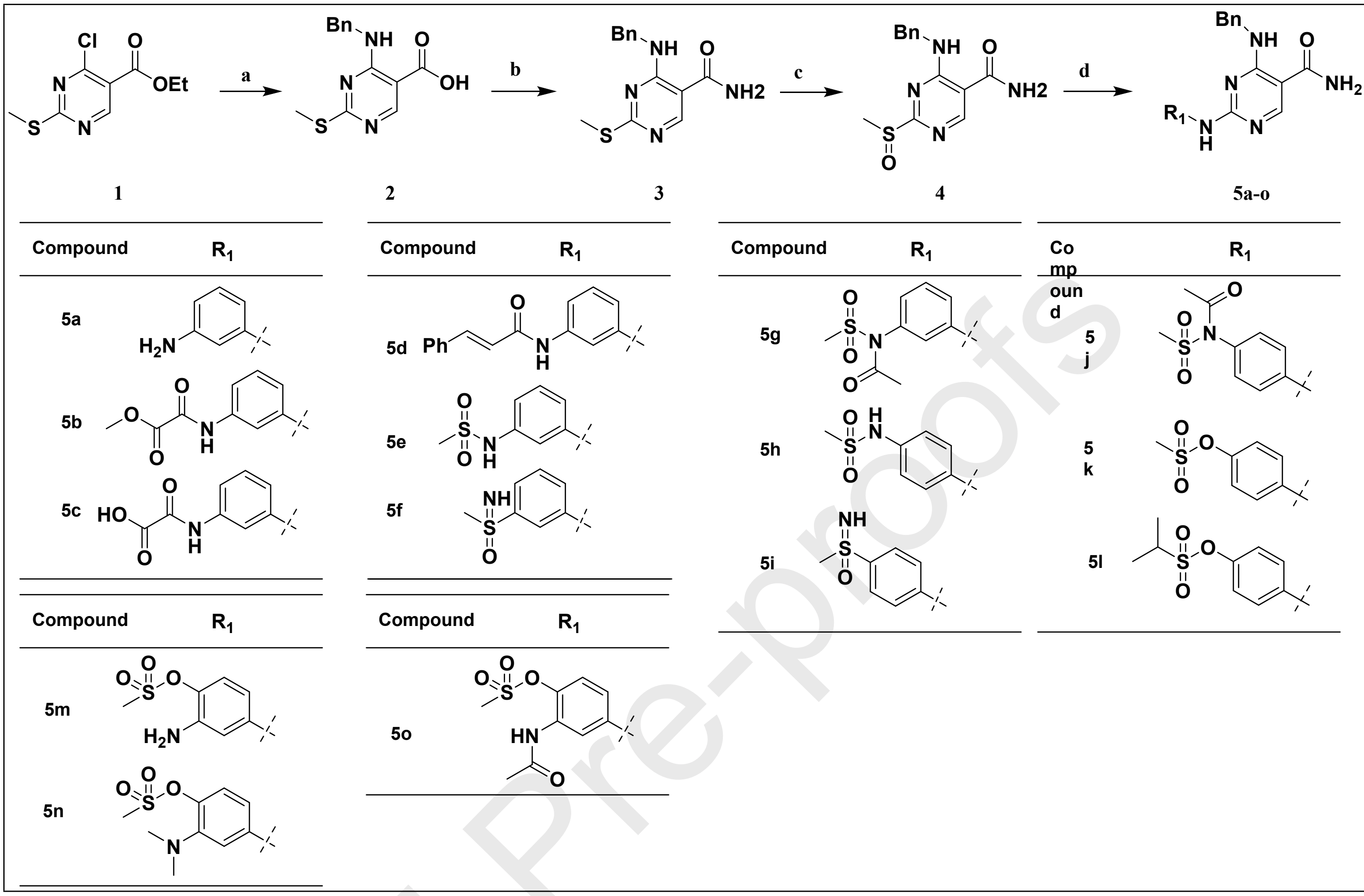

Scheme 1. Synthesis of Compound **5a-o**.

Reagents and conditions: a) Dioxane, DIPEA, Benzyl amine, 26°C, 6h, ii) Dioxane, LiOH, water, 26°C, 6h, 84% b) DMF, EDC.HCl, HOBt, Aq NH_3, 26°C, 1h, 95% c) Dioxane:$CHCl_3$ (1:1), m-CPBA, 50 mins, 10% sodium metabisulfate, 80% d) NMP,PTSA, R_1NH_2, 120°C, 1h.

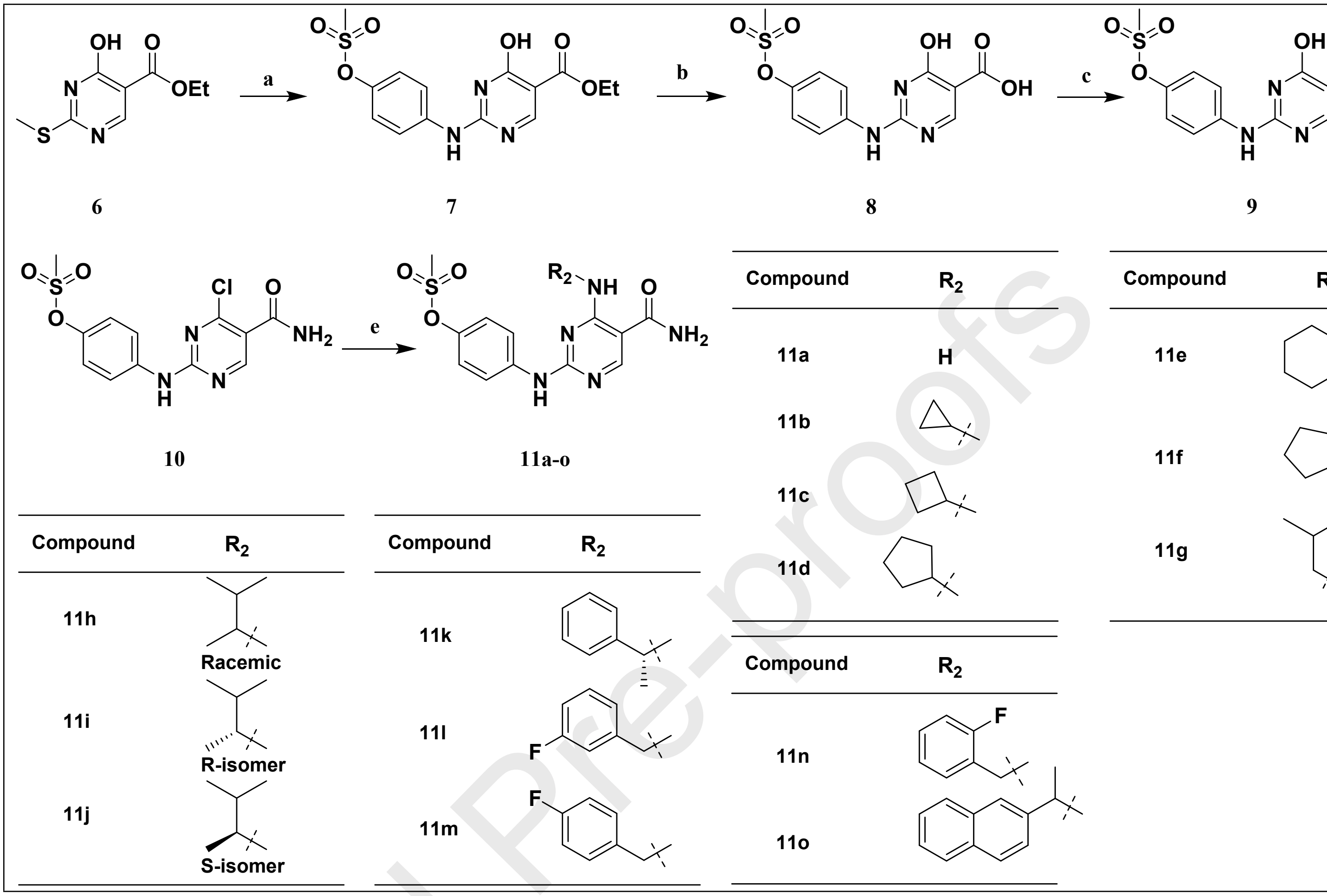

Scheme 2. Synthesis of Compound **11a-o**.

Reagents and conditions: a) (i) Dioxane:$CHCl_3$(1:1), m-CPBA, 50 mins, 10% sodium metabisulfate, 80% (ii) NMP, PTSA, 4-aminophenylmethanesulfonate, 120°C, 1h, 75% b) THF, LiOH, water, 26°C, 6h, 80% c) DMF, EDC.HCl, HOBt, aq NH_3, 26°C, 1h, 70% d) Toluene, $POCl_3$, DIPEA, 120°C, 3 h, 70% e) Dioxane, DIPEA, R_2NH_2, 26°C, 6h.

Table 1 Influence of modification at C2 position of Pyrimidine moiety on JAK3 inhibitory activity (*In vitro*).

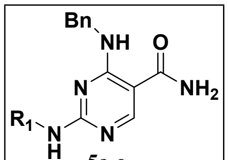

5a-o

Comp.	R_1	JAK-3 IC_{50} (nM)[a]	Comp.	R_1	JAK-3 IC_{50} (nM)[a]
5a	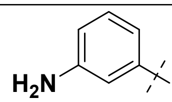	12.6	**5i**	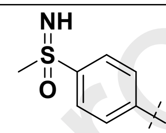	48
5b	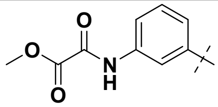	33.4	**5j**	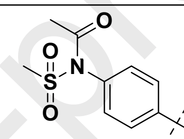	102
5c	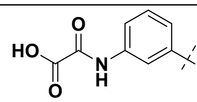	53.7	**5k**	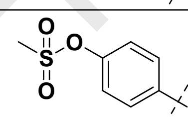	9.5
5d	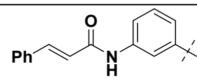	178	**5l**	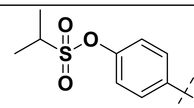	22.4
5e	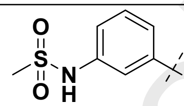	122	**5m**	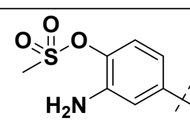	56

5f	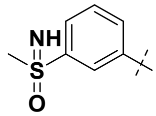	136	**5n**	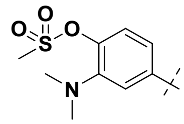	66
5g	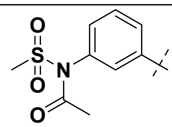	132	**5o**	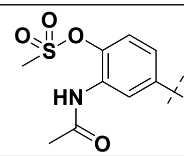	89
5h	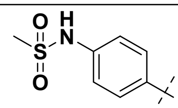	56	**Cerdulatinib**		8
			Tofacitinib		1.6

All the data are shown as the mean for at least two experiments. [a]JAK3 inhibition (IC_{50}) determination using *in vitro* Fluorogenic substrate assays Kit from Millipore.

Table 2 Influence of modification at C4 position of Pyrimidine moiety on JAK3 inhibitory activity (*In vitro*).

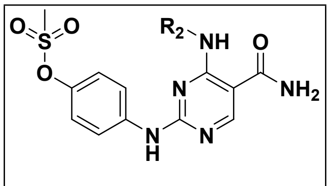

11a-o

Comp.	R_2	JAK-3 IC_{50} (nM)[a]	Comp.	R_2	JAK-3 IC_{50} (nM)[a]
11a	H	300	11i	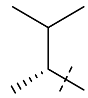 R-isomer	1.7
11b	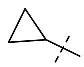	49	11j	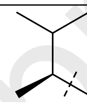 S-isomer	256
11c	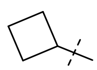	37	11k	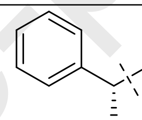	39
11d	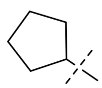	33	11l	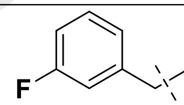	43.2
11e	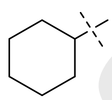	79	11m	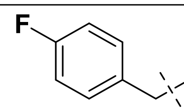	45.4
11f	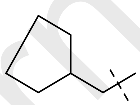	12	11n	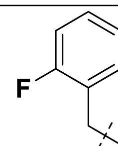	49.2
11g	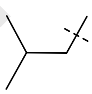	9.8	11o	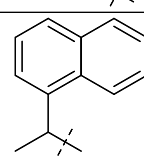	189
11h	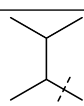 Racemic	20		Cerdulatinib	8
				Tofacitinib	1.6

All the data are shown as the mean for at least two experiments. [a]JAK3 inhibition (IC_{50}) determination using *in vitro* Fluorogenic substrate assays Kit from Millipore.

.

Table 3 *In vitro* isoform selectivity of compounds against JAK1, JAK2 and TYK2 enzymes.

Compound	IC_{50}[a] (nM)				Selectivity fold		
	JAK1[b]	JAK2[b]	JAK3[b]	TYK2[b]	JAK1/ JAK3	JAK2/ JAK3	TYK2/ JAK3
5k	18	42	9.5	45	2	4	5
11i	20	171	1.7	186	12	100	109
Cerdulatinib	15	7	8	5	2	1	<1
Tofacitinib	3	5	1.6	34	2	3	21

[a]The IC_{50} values are shown as the mean for at least two experiments. [b]JAK1, JAK2, JAK3, & TYK2 inhibitory assay Kit (Millipore) was used to screen the test compounds .

.

Table 4: Potency and selectivity determination of **11i** in human PBMC

JAKs involved	**Trigger**	Readout	IC_{50} (nM)		Selectivity	
			11i	Tofacitinib	**11i**	Tofacitinib
JAK1/3	**IL-2**	pSTAT5	22.16	25.22	-	-
JAK1/JAK2/TYK2	**IL-6**	pSTAT3	608	36.88	27.4	1.46
JAK2	**GM-CSF**	pSTAT5	511	210	23	8.32

IC_{50} values in hPBMC were determined by plotting the compound concentration vs the effect on the readouts, using flow cytometry (n=2).

Table 5 Pharmacokinetic study parameters[a] of **5k**, **11i** and Tofacitinib in C57 mice

Compd	Tmax (h)	Cmax (ng/ml)	$t_{1/2}$ (h)	Cl (ml/min/kg), iv	AUC (0-α) h μg/ml	%F*
5k	0.5	146 ± 48	1.85 ± 0.43	40.37 ± 3.61	192 ± 56	15
11i	0.25	1737.95 ± 205	2.56 ± 0.45	11.59 ± 1.65	2104 ± 487	48
Tofacitinib	0.25	80.39± 13.86	1.32 ± 0.65	47.56 ± 3.95	208.2 ± 35.7	20

[a]In male C57BL/6J mice (n=6), compounds were administered orally (po) at 3 mg/kg dose and plasma concentration was analyzed by LC-MS, values indicate Mean ± SD.

* Oral bioavailability (%F) was calculated wrt to iv AUC. Compounds **5k**, **11i** and Tofacitinib administered at 1 mg/kg dose, iv AUC (ng/ml): 412, 1459 and 350 respectively.

Table 6 Hematological parameters and serum chemistry of compound **11i**[a]

Parameters	Compound	
	Control	**11i**[a]
RBC (10^6 μl^{-1})	7.25 ± 0.19	8.35 ± 0.33
AST (U L^{-1})	146.88 ± 11.54	139.71 ± 9.50
TBILI (mg dL^{-1})	0.15.50 ± 0.05	0.18 ± 0.12
WBC (10^3 μl^{-1})	9.10 ± 0.35	8.99 ± 0.30
ALT (U L^{-1})	19.97 ± 1.55	20.69 ± 8.63
ALP (U L^{-1})	135.21 ± 5.78	120.80 ± 12.9

[a] Values expressed as mean ± SD: *n*=9, Male WR dose 100 mg kg^{-1}, po (bid), 14 days repeated dose toxicity study.

Table 7 Relative organ weights (%) after 14 days repeat dose treatment with compound **11i**[a]

Organs	Compounds	
	Control (Vehicle)	**11i**[a] (100 mg kg^{-1}, po, bid)
Brain	0.730±0.028	0.690±0.03
Kidney	0.800±0.034	0.814±0.03
Heart	0.350±0.009	0.360±0.007
Spleen	0.250±0.006	0.243±0.01
Liver	3.598±0.15	3.660±0.078

[a] Values expressed as mean ± SD: *n*=9, Male WR, dose 100 mg kg^{-1}, po (bid), 14 days repeated dose toxicity study.

Table 8 Kinome Selectivity Profile of **11i**[a]

Kinase	%	Kinase	%	Kinase	%
ACK1	12	B-Raf	07	CDK2	10
PKA	13	MAPK1	13	CDK6	02
IR	03	PRK2	20	CDK7	03
Lck	19	IGF-1R	10	CDK9	09
Mer	11	JNK1α1	10	Plk3	03
KDR	00	JNK2α2	05	TAO1	13
SGK	05	PAK4	14	Aurora-A	15
DDR1	18	GCK	19	Aurora-B	19
Syk	00	Pim-1	16	MST1	19
Rsk2	20	Pim-2	05	TBK1	02
ZIPK	00	SAPK2a	01	TrkA	12
Src	09	SAPK2b	07	TrkB	18
ROCK-I	16	SAPK3	09	TrkC	16
ROCK-II	13	SAPK4	02	NEK2	02
FAK	19	MAPKAP-K2	02	Fms	04
STK33	09	Wee1	12	CaMK1	02
JAK3	99.2	MSK1	17	CaMKIIβ	18
Ret	12	Fyn	05	CaMKK2	06
ALK	02	Ab1	03	Lyn	08

ALK4	01	CDK1	09	MEK1	10
Flt1	02	FGFR1	12	PKG1α	19
Flt3	16	DYRK1A	05	GRK5	08
PDGFRα	03	DYRK1B	12	GSK3α	16
CK1	20	CLK2	15	GSK3β	07
MKK4	06	IKKα	02	PKBα	04
MKK6	19	IKKβ	09	PKCθ	17
MKK7β	17	IKKε	01	PKCξ	10

.[a]Values represent percent inhibition at 1 µM concentration, listed key 91 kinase as representative data as mean of 2 independent measurements. Higher numbers indicate stronger binding, DMSO used as negative control (% inhibition=0%).

Highlights

Discovery of Diaminopyrimidine-carboxamide Derivatives as JAK3 Inhibitors

1) Selective inhibition of janus kinase (JAK) has been identified as an important strategy for the treatment of autoimmune disorders.

2) Optimization at the C2 and C4-positions of pyrimidine ring of Cerdulatinib led to the discovery of a potent and orally bioavailable 2,4-diaminopyrimidine-5-carboxamide based JAK3 selective inhibitor (**11i**).

3) A cellular selectivity study further confirmed that **11i** preferentially inhibits JAK3 over JAK1, in JAK/STAT signaling pathway.

4) Compound **11i** showed good anti-arthritic activity, which could be correlated with its improved oral bioavailability.

5) In the repeat dose acute toxicity study, **11i** showed no adverse changes related to gross pathology and clinical signs, indicating that the new class JAK3 selective inhibitor could be viable therapeutic option for the treatment of rheumatoid arthritis.

Graphical Abstract

Discovery of Diaminopyrimidine-carboxamide Derivatives as JAK3 Inhibitors